

**Studies on autophagy during the embryonic
and early neonatal periods**

Makoto Matsui

DOCTOR OF PHILOSOPHY

Department of Basic Biology

School of Life Science

The Graduate University for Advanced Studies

2006

Acknowledgements

I wish to express my deepest appreciation to Professor Yoshinori Ohsumi for giving me a chance of this study in his laboratory, for his extensive advices and insightful discussion throughout this study. I wish also to express my gratitude to Dr. Noboru Mizushima (Protein Metabolism Project, The Tokyo Metropolitan Institute of Medical Science) for his constant supervision, extensive advice, insightful discussion and encouragement throughout this study. I would like to gratefully thank Dr. Akiko Kuma (Protein Metabolism Project, The Tokyo Metropolitan Institute of Medical Science) for her advice and profound discussion. I am grateful to Dr. Akitsugu Yamamoto (Department of Bio-Science, Nagahama Institute of Bio-Science and Technology) for his excellent electron microscopic analysis. I also thank Professor Yoshinori Ohsumi's laboratory members (and past members), such as Dr. Yoshiaki Kamada, Dr. Takeshi Noda, Dr. Kuninori Suzuki, Dr. Yukiko Kabeya, Dr. Takayuki Sekito, Dr. Kohki Yoshimoto, Dr. Takao Hanada, Dr. Yuki Fujiki, Dr. Maho Hamasaki, Dr. Jun Onodera, Dr. Mamoru Ohneda, Dr. Hitoshi Nakatogawa, Dr. Hisashi Ichikawa, Tomoko Kawamata, Takuya Kageyama, Yoko Hara, Kumi Tsukeshiba, Masami Miwa for their continuous support and good company along my stay in National Institute for Basic Biology. I wish to express my appreciation to other members) and past members) of Dr. Noboru Mizushima's laboratory, such as Dr. Taichi Hara, Dr. Jun sunayama, Dr. Eiko Oita, Dr. Takumi Kanazawa, Nao Hosokawa, Hiroyuki Neko, Yuko Mitani, Kumiko Uchiyama, Guillermo Mariño, Zijiang Zhao for their continuous support and good company along my stay in The Tokyo Metropolitan Institute of Medical Science.

January 10, 2006

Makoto Matsui

Table of contents

Summary • • • • •	1
Introduction • • • • •	3
<i>Protein degradation in eukaryote</i>	3
<i>Lysosome/vacuole protein transport</i>	3
<i>Autophagy</i>	4
<i>Autophagy pathway</i>	4
<i>Molecular mechanism of autophagy</i>	6
<i>Response to starvation</i>	8
<i>Role of basal autophagy</i>	11
<i>Cell death and autophagy</i>	11
<i>Organelle degradation and autophagy</i>	12
<i>Aim of this issue</i>	12
Materials and methods • • • • •	14
<i>Antibodies</i>	14
<i>Mouse</i>	14
<i>Artificial feeding</i>	14
<i>Observation of GFP-LC3 transgenic mice tissues</i>	14
<i>Quantification of GFP-LC3 dots</i>	15
<i>Immunofluorescence and immunohistochemical analysis</i>	15
<i>Detection of cell death by TUNEL (TdT-mediated dUTP-biotin Nick End Labeling) method</i>	16
Results • • • • •	17
<i>Autophagy was extensively induced in various tissues after natural birth</i>	17
<i>Autophagy occurs constitutively active in the thymus</i>	18
<i>GFP-LC3 is aggregated in neonatal hepatocytes in Atg5^{-/-} mice</i>	18
<i>Accumulation of IBs in Atg5^{-/-} mice</i>	19
<i>Normal cell death in autophagy-deficient mice</i>	20
<i>Organelle degradation in lens fiber cells occurs normally</i>	21

Discussion • • • • •	23
<i>Induction of autophagy in neonatal period</i>	23
<i>Constitutively active autophagy</i>	24
<i>Intracellular clearance by constitutive autophagy</i>	24
<i>Mechanism of Ub-positive aggregate formation</i>	26
<i>Relevance to pathophysiology of neurodegeneration</i>	27
<i>Organelle degradation in lens fiber cells</i>	28
 References • • • • •	 44

List of figures

Figure 1. A schematic overview of autophagy steps	5
Figure 2. Diagram of the autophagosome formation	7
Figure 3. Autophagy in muscle tissues in adult	10
Figure 4. Localization of GFP-LC3 in the heart of embryos and neonates mice	29
Figure 5. Localization of GFP-LC3 in various tissues of embryos and neonates	30
Figure 6. Autophagy is induced in various neonatal tissues	32
Figure 7. Quantification of GFP-LC3 dots in neonatal tissues	33
Figure 8. Localization of GFP-LC3 in the thymus of embryos and adults	34
Figure 9. Localization of GFP-LC3 in the brain of embryos and neonates	35
Figure 10. Electron microscopic analysis of the hearts from wild-type neonates	36
Figure 11. LC3 dot structures in Atg5 ^{-/-} represent IBs	37
Figure 12. Ubiquitin-positive IBs accumulate in Atg5 ^{-/-} tissues	38
Figure 13. Immunoelectron micrograph of ubiquitin-positive IBs	39
Figure 14. Normal cell death in autophagy-deficient mice	40
Figure 15. Localization of GFP-LC3 in embryonic lens	41
Figure 16. Normal OFZ formation in lens of Atg5 ^{-/-} mice	42
Figure 17. Roles of induced and baseline autophagy	43

Summary

Autophagy is a non-selective degradation process in which long-lived proteins and organelles are sequestered within double-membrane vesicles, termed autophagosomes that deliver the contents to the lysosome/vacuole for degradation. The lysosome/vacuole is an acidic compartment that contains various hydrolytic enzymes. Autophagy is fundamental and evolutionarily conserved function in eukaryotes. More than 20 genes, which are essential for autophagy (*ATG* genes; AuTophagGy), have been identified by genetic screens in yeast, and most of the *ATG* genes are conserved in higher eukaryotes.

The major function of autophagy is response to starvation. For example, autophagy is suppressed to undetectable levels under nutrient rich conditions in yeast, but it is rapidly induced under nutrient starvation conditions. In autophagy deficient mutants of yeast, the survival rate decreases under starvation conditions. Similarly, autophagy also plays a response to starvation in mammals. Autophagy is induced in many tissues in response to food withdrawal in adult mice. Autophagy-defective mutant mice, *Atg5^{-/-}* mice, appear almost normal at birth, but most of the *Atg5^{-/-}* neonates died within 1 day of delivery. I thought that phenotype of *Atg5^{-/-}* mice is related to nutrient starvation. However, the kinetics of autophagy is unclear in wild-type embryos and neonates. In this study, to study the significance of mammalian autophagy *in vivo*, I observed occurrence of autophagy in embryos and neonates using transgenic mouse model in which autophagosomes are labelled with GFP-LC3.

I observed that autophagy remained at low levels throughout the embryonic period. Formation of autophagosomes was extensively induced in various tissues after a natural birth and is maintained at high levels for 3-12 h after birth. The number of autophagosomes gradually decreased to basal levels by day one or two. Soon after birth, mammals face with the first, and probably the most severe, starvation during their lifespan, because trans-placental nutrients supply is suddenly terminated. These results suggest that induction of autophagy is important for survival during neonatal starvation.

In mammal, embryos are under the nutrient rich conditions. However, I observed that low levels of autophagy occur constantly at embryonic period. It is

unclear that the basal autophagy plays an important role during mouse embryogenesis. In this study, I examined the role of basal autophagy using the autophagy indicator mice and autophagy deficient mice. In histological examination of *Atg5^{-/-}* neonates, I detected ubiquitin-positive aggregates (inclusion bodies; IBs) only in a few tissues, including neural cells, hepatocytes, and anterior pituitary gland cells. These results suggest that function of autophagy is not only maintenance of viability during starvation, but also intracellular quality control. Recently, a similar observation was reported in the hepatocytes of liver-specific conditional *Atg7^{-/-}* mice. I demonstrated that time from the liver genesis to the birth is sufficient to generate large IBs in hepatocytes. In addition, I revealed that protein quality control is highly dependent on basal levels of autophagy in hepatocytes, neural cells and anterior pituitary cells.

Autophagy can degrade not only proteins but also intracellular organelles such as mitochondria, peroxisomes and endoplasmic reticulum. Dramatic degradation of organelles is observed in the processes of lens organelle free zone (OFZ) formation. The mechanism by which these organelles are destroyed during this process is not fully understood. It is suggested that autophagy is involved in lens organelle degradation. However, organelle degradation during the differentiation of lens occurred normally in *Atg5^{-/-}* mice. Therefore, autophagy is dispensable for OFZ formation in lens epithelial cells.

In this study, I showed significance of basal- and induced-autophagy during embryogenesis and neonatal starvation. These findings of *in vivo* analyses will help to understand physiological significance of autophagy in mammals.

Introduction

Protein degradation in eukaryote

Cell homeostasis is maintained by precisely regulated balance between synthesis and degradation of cellular components. In eukaryotic cells, intracellular proteins are degraded by two major processes; the ubiquitin-proteasome and the lysosome/vacuole pathway. The ubiquitin-proteasome pathway selectively degrades most intracellular short-lived, damaged or misfolded proteins (Hochstrasser, 1996; Hershko and Ciechanover, 1998). In this pathway, proteins are targeted for degradation by covalent ligation to ubiquitin, a highly conserved small protein. On the other hand, long-lived proteins and some cytoplasmic organelles are degraded within a specific compartment, the vacuole in yeast and the lysosome in mammalian cells (Klionsky and Ohsumi, 1999).

Lysosome/vacuole protein transport

The lysosome/vacuole is the major catabolic compartment in eukaryotic cells and contains a range of hydrolases capable of degrading most cellular constituents. This organelle is the terminal destination for endocytic, autophagic and secretory materials targeted for destruction. There are at least three different pathways for vacuole transport of cytosolic contents in yeast: Cvt (cytosol to vacuole targeting pathway) (Scott *et al.*, 1996), Vid (vacuolar import and degradation pathway) (Shieh *et al.*, 1998) and autophagy pathway (Takeshige *et al.*, 1992). The Cvt and Vid pathway are found only in yeast. In the Cvt pathway, two vacuolar proteins, aminopeptidase I and α -mannosidase, are selectively transported to vacuoles. Under nutrient-rich conditions, this process is mediated by an autophagosome-like structure called a Cvt vesicle. In the Vid pathway, the gluconeogenic enzyme fructose-1, 6-bisphosphatase (FBPase) is rapidly degraded following a shift from low glucose condition to high glucose conditions. FBPase trafficks from the cytosol to the vacuole via Vid vesicles. Only autophagy pathway is an evolutionarily conserved process that occurs in virtually all eukaryotic cells, ranging from yeast to mammals

Autophagy

Autophagy (from Greek auto, self, and phagos, to eat) was first described ultrastructurally as the sequestration of cytoplasm into closed, membrane-delimited vacuoles called autophagosome (de Duve and Wattiaux, 1966). Autophagy has three major pathways, chaperon-mediated autophagy (Schworer *et al.*, 1981; Mortimore *et al.*, 1989; Dunn, 1994), microautophagy (Ahlberg and Glaumann, 1985; Mortimore *et al.*, 1988) and macroautophagy (Dice, 1990; Seglen and Bohley, 1992). Chaperon-mediated autophagy is the process in which substrates to be degraded are translocated across the lysosome/vacuole. Microautophagy, degradation substrates are engulfed by lysosome/vacuole directly. By contrast, macroautophagy (hereafter simply referred to as autophagy) is the main route to lysosomes/vacuole. Substrates are nonselectively encompassed by autophagosomes and delivered to lysosomes/vacuole.

Autophagy pathway

Autophagy is a membrane trafficking process that transports bulk cytoplasm and entire organelles to the lysosome (Figure 1). Autophagy is found ubiquitously in eukaryotes and involved in amino acids production, prevention of disease and aging (including removal of damaged organelles), regulation of metabolism and developmental pathway. Although autophagy occurs constitutively, it is induced under both extracellular stress conditions (nutrient deprivation, hypoxia) (Mortimore and Poso, 1986) and intracellular stress conditions (accumulation of damaged organelles, protein aggregated) (Ravikumar and Rubinsztein, 2004). The initial event in autophagy, triggered, for example, by nutrient starvation and hormones (such as glucagons) (Mortimore and Schworer. *et al.*, 1975) is the sequestration and enclosure of a piece of cytoplasmic constituents, including organelles such as mitochondria, by one or more specialized membrane cisternae of uncertain origin, called isolation membrane. Closure of the isolation membrane results in formation of double membrane structures, called autophagosomes or initial autophagic vacuoles (AVi). Autophagosomes then fuse with endosomes, and eventually fuse with lysosomes to become autolysosomes or degradative autophagic vacuoles (AVd). Lysosomal hydrolases degrade the

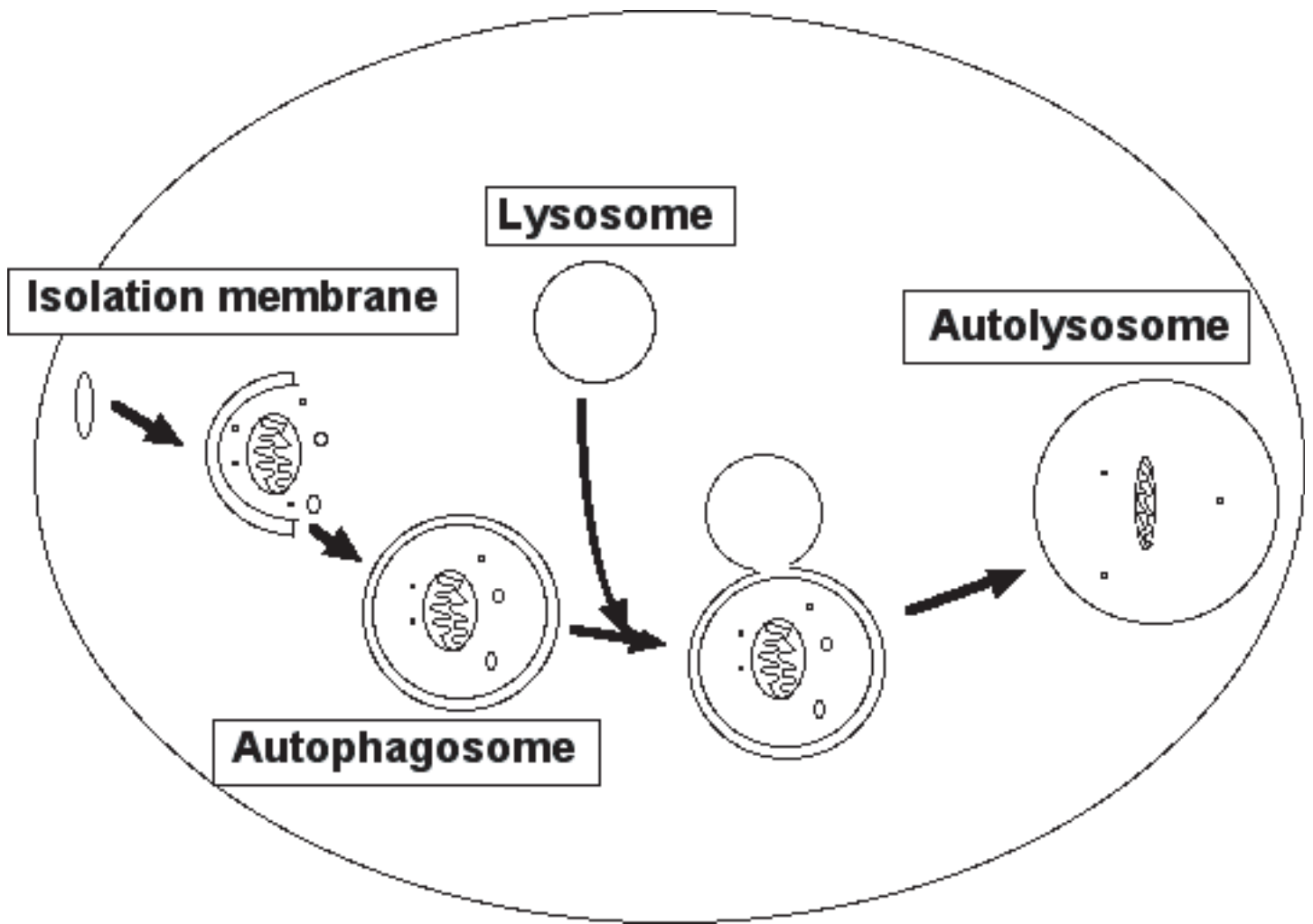


Figure 1. A schematic overview of autophagy steps

Autophagy is a membrane trafficking process. Cytosol and organelles are enwrapped by membrane, termed isolation membrane. Afterwards, a double-membrane vesicle, the autophagosome, is formed. The autophagosome acquires hydrolytic enzymes by fusing with the lysosome to generate an autolysosomes, and the inner vesicle of autophagosome is released into the lumen. The resulting autophagic body is broken down.

cytoplasm-derived components of the autophagosome, together with its inner membrane.

Molecular mechanism of autophagy

Yeast genetic studies have identified more than 20 genes (AuTophGy: *ATG* genes) required for autophagy, most of which function in autophagosome formation (Klionsky *et al.*, 2003). Included in this group are two sets of components involving ubiquitin-like (Ubl) protein conjugation systems that are essential for autophagosome formation (Ohsumi, 2001). The first Ubl is Atg12, which is covalently attached to Atg5 (Mizushima *et al.*, 1998; Mizushima *et al.*, 2001; Mizushima *et al.*, 2003). The C-terminal glycine residue of Atg12 is activated by Atg7 in ATP-dependent manner. Atg12 is then transferred to Atg10 to form a thioester again. The function of Atg10 likely is equivalent to that of E2 ubiquitin-conjugation enzymes. The C-terminal glycine of Atg12 is covalently attached to lysine 149 of Atg5 via an isopeptide bond. The second Ubl is Atg8, called LC3 in mammals, that undergoes proteolytic processing prior to modifying the lipid phosphatidylethanolamine (PE) (Ichimura *et al.*, 2000; Kirisako *et al.*, 2000). Following synthesis, the C-terminus of Atg8 is cleaved by a cysteine protease, Atg4, leaving a glycine residue at C terminus. Cleaved Atg8 is activated by an E1 protein, Atg7, which is shared with the Atg12 system. Atg8 is transferred subsequently to E2 enzyme Atg3. Atg8 is modified by PE on the C-terminus (LC3-II form) and binds tightly to autophagosomal membrane.

Formation of the Atg12-Atg5 conjugate is essential for proceeding of autophagy. The covalent modification of Atg5 with Atg12 is essential for elongation of the isolation membranes (Mizushima *et al.*, 2001; see Figure 2). It was observed that Atg12-Atg5 conjugate initially associates with a small crescent-shaped vesicle evenly in mammalian cells. As the membrane elongates, Atg12-Atg5 associates with the outer side of the membrane asymmetrically. Finally, Atg12-Atg5 dissociates from the membrane upon completion of autophagosome formation. Furthermore, this conjugate is required for targeting of Atg8 to the isolation membranes. LC3, a mammalian homologue of yeast Atg8, was shown to localize on autophagosome membrane (Kabeya

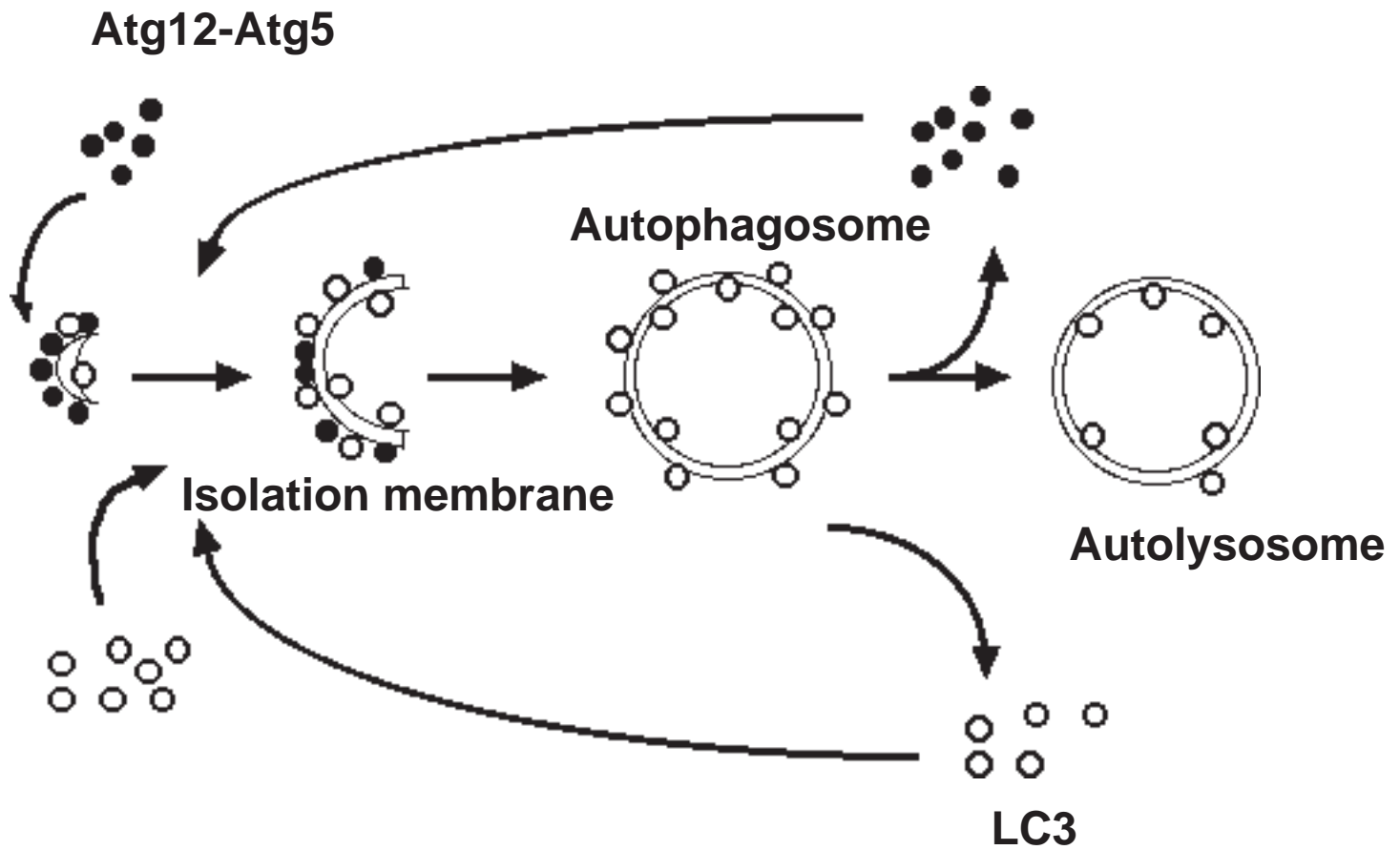


Figure 2. Diagram of the autophagosome formation

Atg12-Atg5 conjugates initially associates with a small crescent-shaped vesicle evenly. When the membrane elongates, this conjugates associates with the outer side of the membrane asymmetrically. Finally, this conjugates dissociates with the membrane upon completion of autophagosome formation. LC3 was shown to localize on autophagosome membrane. LC3 remains on autophagosome even after Atg12-Atg5 conjugate dissociates. Dissociated Atg12-Atg5 and LC3 are reused, its associates with other isolation membrane again.

et al., 2000). LC3 remains on autophagosome even after Atg12-Atg5 conjugate dissociates, so that it is used as an autophagosome marker.

Response to starvation

In yeast, autophagy is suppressed to undetectable levels under growing conditions, but it is rapidly (within 30 min) induced during nitrogen starvation (Takeshige *et al.*, 1992). Autophagy was first discovered under nitrogen starvation condition in the yeast. Then carbon, sulfate, phosphate, and even single auxotrophic amino acid depletion were also shown to induce the same membrane dynamics, although the extent of the response varied. Autophagy mutants of yeast have defect in bulk protein degradation in vacuoles during starvation. Furthermore, mutants lost its viability faster than wild-type cells in starvation conditions. The critical role played by autophagy in maintaining viability during starvation has been shown in several species, such as *S. cerevisiae* (Tsukada and Ohsumi, 1993), *D. discoideum* (Otto *et al.*, 2003; Otto *et al.*, 2004), *D. melanogaster* (Scott *et al.*, 2004) and *C. elegans* (Melendez *et al.*, 2003).

A number of developmental defects have been also found in autophagy mutants in several species. In *S. cerevisiae*, autophagy mutants are defective in spore formation (Tsukada and Ohsumi, 1993). Atg1, Atg5 and Atg7 mutants of *D. discoideum* are not grossly affected in growth, but survival during nitrogen starvation is severely reduced (Otto *et al.*, 2003; Otto *et al.*, 2004). Bulk protein degradation during starvation-induced development is reduced in the autophagy mutants. Moreover, development is aberrant; the autophagy mutants do not aggregate in plaques on bacterial lawns, but they do proceed further in development on nitrocellulose filters, forming defective fruiting bodies. Premature death from the third larval to pupal stages was reported in *D. melanogaster* mutants (Scott *et al.*, 2004; Juhasz *et al.*, 2003; Baehrecke 2003). Draut1, the *Drosophila* homolog of yeast Atg3, loss of function larvae is unable to induce autophagy in fat body cells before pupariation and die during metamorphosis (Juhasz *et al.*, 2003). In wild-type, massive autophagy is observed in dying larval tissues such as the salivary glands (Baehrecke, 2003). In *Drosophila*, the mutant third larvae

leave food sources and starve as a result. During the pupal stage, larval tissues are degraded and used as nutrients to generate adult tissues. Dauer formation is abnormal in *C. elegans* autophagy mutants (Melendez *et al.*, 2003). Using nematodes with a loss-of-function mutation of *bec-1*, the *C. elegans* ortholog of the yeast and mammalian autophagy gene *ATG6/VPS30/beclin1*, is essential for normal dauer morphogenesis and life span extension. Dauer formation is associated with increased autophagy. These reports raise the possibility that these developmental defects of autophagy mutants reported in various species are related to nutrient starvation (Tsukada and Ohsumi, 1993; Otto *et al.*, 2003; Juhasz *et al.*, 2003; Scott *et al.*, 2004; Melendez *et al.*, 2003).

In mammalian cells, autophagy is also induced by nutrient starvation (Meijer and Codogno, 2004). Recently, Mizushima *et al.* have developed an autophagy indicator mouse model, in which autophagosomes are labeled with LC3 fused to green fluorescent protein (GFP) (Mizushima *et al.*, 2004; Mizushima, 2004). Through a systematic analysis of this mouse model, autophagy was found to be activated in almost all organs following initiation of starvation *in vivo* (Figure 3). These findings suggest that autophagy in mammals also plays an important role in maintaining viability during starvation conditions in adult mice (Mizushima *et al.*, 2004). Kuma *et al.* determined the significance of autophagy by analyzing mice deficient in *Atg5*, a gene essential for elongation of the isolation membrane (Mizushima *et al.*, 2001). *Atg5*^{-/-} mice appear almost normal at birth, but most of the *Atg5*^{-/-} neonates died within 1 day of delivery (Kuma *et al.*, 2004). It is known that neonates face with nutrient limitation, because neonates are suddenly terminated trans-placental nutrient supply (Medina *et al.*, 1992). However, the kinetics of autophagy is unclear in the mammalian embryos and neonates. The aim of this study is to determine whether autophagy occurs in embryos and neonates. I will reveal that how much autophagy occurs in the mammalian embryonic and neonatal period.

Role of basal autophagy

It is known that autophagy is a non-selective protein degradation process, and it degrades long-lived proteins and organelles (including abnormal proteins and

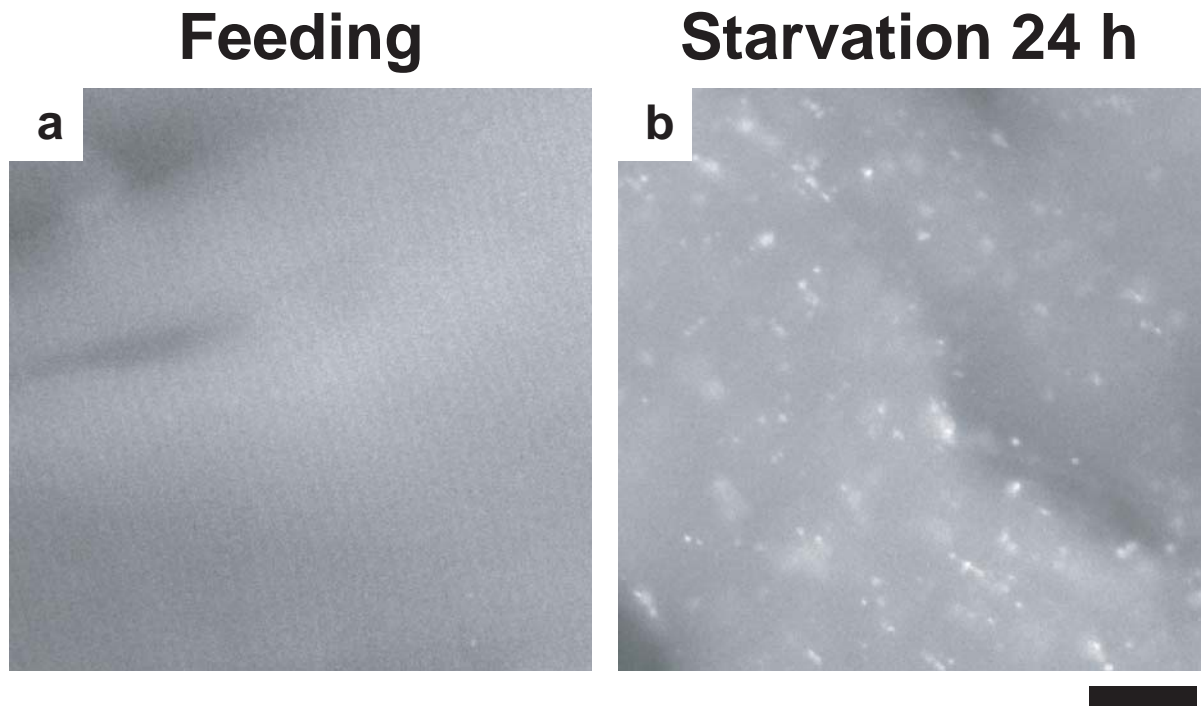


Figure 3. Autophagy in muscle tissues in adult

GFP images of extensor digitorum longus (EDL) muscle of GFP-LC3 mice following (A) 0-, (B) 24-h starvation. Bar, 10 μ m.

damaged organelles). Autophagy-defective yeast cells (Tsukada and Ohsumi, 1993), embryonic stem (ES) cells (Mizushima *et al.*, 2001) and embryonic fibroblasts (Kuma *et al.*, 2004) are quite healthy and show no apparent abnormalities under growing conditions. Recently, the hepatocytes of liver-specific conditional *Atg7^{-/-}* mice develop ubiquitin-positive aggregates (inclusion bodies; IBs) (Komatsu *et al.*, 2005). These results suggest that function of autophagy is not only as maintenance of viability during starvation, but also as an intracellular quality control system.

It is thought that the embryos are not starved, because nutrients are provided through the placenta from mothers. Accordingly, autophagy would play a role independent from its function in starvation adaptation. In this study, I analyzed autophagy deficient mice embryos and neonates to discover that the basal autophagy is an important mechanism for intracellular clearance during embryogenesis.

Cell death and autophagy

It has been reported that autophagy may be also involved in cell death. It is now apparent that there are several types of programmed cell death other than typical apoptosis. One type, the so called ‘autophagic cell death’ or ‘type 2 cell death’, is characterized by the appearance of cytoplasmic vacuoles, which are thought to be related to autophagy (Baehrecke, 2003; Gozuacik and Kimchi, 2004). In classical apoptotic or Type 1 programmed cell death, there is early collapse of cytoskeletal elements, but preservation of cytoplasmic organelles until late in the process. In contrast, in autophagic or Type 2 cell death, there is early degradation of cytoplasmic organelles by autophagy, but preservation of cytoskeletal elements until late stages, presumably because of their role in autophagy (Bursch *et al.*, 2004; Clarke, 1990). However, it is unclear that whether autophagy acts fundamentally as a cell survival or cell death pathway or both. It is known that the cell death has occurred actively during embryogenesis. In this study, I determined whether cell death is up regulated in the absence of autophagy.

Organelle degradation and autophagy

In contrast to the ubiquitin-proteasome system, autophagy can degrade not only proteins but also intracellular organelles such as mitochondria (Takeshige *et al.*, 1992; Rodriguez-Enriquez *et al.*, 2004), peroxisomes (Tuttle *et al.*, 1995; Sakai *et al.*, 1998) and endoplasmic reticulum (Masaki *et al.*, 1987; Hamasaki *et al.*, 2005). Some of these organelles are recognized selectively (Tuttle *et al.*, 1995; Sakai *et al.*, 1998). Moreover, abnormal organelles were observed in autophagy-deficient hepatocytes, suggesting that autophagy might be involved in quality control of intracellular organelles (Komatsu *et al.*, 2005).

In addition to the normal turnover of intracellular organelles, dramatic degradation of organelles is observed in the processes of lens and erythroid development. The lens contains two types of cells, the epithelial cells covering the anterior surface of the lens and the fiber cells that differentiate from the epithelial cells. During late embryogenesis, organelles within the epithelial cells are rapidly lost, which allows fiber cells to be transparent (David and Shearer, 1989; McAvoy *et al.*, 1999; Bassbett, 2002). Similarly, intracellular organelles are eliminated during erythroid cell maturation. The mechanism by which these organelles are destroyed during this process is not fully understood. The presence of autophagic vacuoles in these cells during differentiation suggested the involvement of autophagy in the organelle loss (Tooze and Davies, 1965; Kent *et al.*, 1966; Walton and MacAvoy, 1984; Heynen *et al.*, 1985; Takano-Ohmuro *et al.*, 2000). Therefore I addressed this issue using autophagy-indicator mice (Mizushima *et al.*, 2004) and autophagy-deficient mice (Kuma *et al.*, 2004).

Aim of this issue

As described above, autophagy plays important roles as starvation response. Autophagy-defective mutant mice, *Atg5*^{-/-} mice, appear almost normal at birth, but most of the *Atg5*^{-/-} neonates die within 1 day of delivery. It is unclear how much autophagy occurs in mammalian embryos and neonates. I have two questions. One; how much does autophagy occur in the embryonic and the neonatal period?

Another important question; what is the role of basal autophagy? Autophagy is

a non-selective protein degradation process, and it degrades long-lived proteins and organelles (including abnormal proteins and damaged organelles). If abnormal proteins accumulate in the cell, the cells will be damaged. Consequently, I thought that intracellular clearance by autophagy is very important. In the embryonic period, it is not necessary to consider about induced autophagy, because the nutrient condition is not limited in embryos.

In this study, I analyzed significance of autophagy in embryos and neonates by using autophagy indicator mice and autophagy deficient mice. I observed that autophagy was transiently induced after birth. I also found an important role for basal autophagy in constitutive turnover of intracellular components, and loss of autophagy resulted in accumulation of ubiquitinated proteins. This study will help to understand the physiological significance of autophagy during embryogenesis and neonatal survival.

Materials and methods

Antibodies

An antibodies against recombinant rat LC3b (anti-LC3#1) was generated as described (Kabeya et al., 2000). A polyclonal anti-GFP antibody and AlexaFluor 488- and 660-conjugated goat anti-rabbit IgG (H+L) antibodies were purchased from Molecular Probes. A mouse monoclonal anti-ubiquitin antibody (1B3), purchased from Medical & Biological Laboratories (MBL), was used histochemistry. A rabbit polyclonal antibody against ubiquitin, used for immunoelectron microscopy, was purchased from DakoCytomation. A mouse anti-KDEL monoclonal antibody was purchased from Stressgen.

Mouse

All mice were C57BL/6 background. *Atg5*^{+/-} mice were interbred to obtain *Atg5*^{-/-} mice. *Atg5*^{-/-} mice were crossed with GFP-LC3 transgenic mice to produce *Atg5*^{-/-} mice expressing GFP-LC3 (*Atg5*^{-/-} GFP-LC3/+). For caesarian delivery, pregnant mother were injected on 17.5 day post conception (dpc) and 18.5 dpc with 2 mg progesterone (luteum injection, Teikoku Hormone Mfg. Co.) obtained at 19.5 dpc. All animal experiments were approved by institutional committees of the Tokyo Metropolitan Institute of Medical Science.

Artificial feeding

Newborn pups were obtained by caesarean delivery at 19.5 dpc and placed in a humidified, thermostat-controlled chamber (30°C). For artificial milk feeding, a fine tube was inserted into the stomach, and 30 µl of 0.13 mg/ml infant formula for human neonates (Haihai, Wakodo Co.) was fed through the tube every 3-6 h.

Observation of GFP-LC3 transgenic mice tissues

Tissue sample for GFP-LC3 observation were prepared from E13.3 to neonate, and fixed with 4% paraformaldehyde (PFA) in 0.1 M sodium phosphate buffer (PB; pH

7.4) for at least 12 h, followed by treatment with 15% sucrose in phosphate-buffered saline (PBS; pH 7.4) and then with 30% sucrose solution overnight. Tissue samples were embedded in Tissue-Tek O.C.T. compound (Sakura Finetechnical Co., Ltd., Tokyo, Japan) and stored at -80 °C. The samples were sectioned at 5 µm thickness with cryostat (CM3050 S, Leica, Deepfield, IL), air-dried for 30 min, and stored at -80 °C until use. Cryosections were washed with PBS for 5 min and air-dried for 10 min. Samples were mounted using SlowFade Light Antifade Kit. (Molecular Probes Inc.). The mounted sections were directly observed by a fluorescence microscope (Olympus IX81, Tokyo, Japan) equipped with a CCD camera (ORCAER, Hamamatsu Photonics, Hamamatsu, Japan). U-MGFPHQ mirror unit (Olympus IX81, Tokyo, Japan), which is dichromatic mirror, was used for GFP observation and U-MWIG2 mirror unit (Olympus IX81, Tokyo, Japan) was used to check autofluorescence.

Quantification of GFP-LC3 dots

Cryosections were prepared from tissues isolated at the E18.5, postnatal day (P) 0, 0.5 h, 3 h, 6 h, 12 h, 24 h and P 2.5. The ratio of the total area of GFP-LC3 dots to the total cellular area is shown as percentage. These analyses were analyzed with software named MetaMorph (Universal Imaging Co.).

Immunofluorescence and immunohistochemical analysis

For immunofluorescent microscopy, mice were fixed with 4% PFA for overnight, and tissues were removed and immersed in sucrose solution or in 70% Ethanol for paraffin embed. Cryosections were prepared as described above. Paraffin samples were embedded in paraffin with universal manner. Paraffin sections were deparaffinized with xylene and dehydrate in a graded series of ethanol (absolute, 95%, 90%, 80%, 70%, diluted in distilled water) and were rinsed well with PBS for 5min, 3 times. After rehydrate, cryo- and paraffin-sections were treated with microwave in 0.01 M citrate buffer/0.01 M Na₂HPO₄ buffer for 10 min and cool down to room temperature. After blocking with 5% bovine serum albumin (BSA) in PBS, sections were incubated with primary antibody for 1h, followed by 30 min incubation of 2nd

antibody. Samples were mounted using SlowFade Light Antifade Kit. (Molecular Probes Inc.).

For immunohistochemical analysis, antigen activated samples were treated with 0.3% H₂O₂/methanol for intrinsic peroxidase inactivation. After blocking with BEAT Blocking Solution (Histomouse-Plus Kit; Zymed Laboratories Inc.), sections were incubated with primary antibody for 1 h. Sections were followed by addition of biotinylated secondary antibody, which serves as a linker between the primary antibody and the streptavidin-peroxidase conjugate. The presence of peroxidase can be revealed by addition of DAB substrate-chromogen solution.

Detection of cell death by TUNEL (TdT-mediated dUTP-biotin Nick End Labeling) method

Paraffin sections were prepared as described above. After rehydrate, paraffin sections were treated with 20 mg/ml proteinase K, nuclease free, in 10mM Tris-HCl, pH 7.6, for 15 min at 37°C. Cell death was detected by In Situ Cell Death Detection Kit, Fluorescein (Roche Diagnostics) according to the appended protocol. Samples were mounted using SlowFade Light Antifade Kit. (Molecular Probes Inc.). The mounted sections were directly observed by a fluorescence microscope (Olympus IX81, Tokyo, Japan) equipped with a CCD camera (ORCAER, Hamamatsu Photonics, Hamamatsu, Japan). U-MGFPHQ mirror unit (Olympus IX81, Tokyo, Japan).

Results

Autophagy was extensively induced in various tissues after natural birth

Mizushima *et al.* generated a transgenic mouse model in which autophagosomes were labelled with GFP-LC3 in almost all tissues. LC3 is one of the mammalian proteins homologous to yeast Atg8. In this mouse model, it was observed that autophagy was induced in many tissues in response to food withdrawal in young to adult mice. To study the kinetics of mammalian autophagy during development, I observed GFP-LC3-labelled structures (GFP-LC3 ‘dots’) in the embryonic and perinatal stages (Fig. 4, Fig. 5 and Fig. 6). First, I observed heart, because autophagy is massively increased following food withdrawal in heart of adult mice (Mizushima *et al.*, 2004). In day 13.5 embryos, I detected a small, but significant, number of GFP-LC3 dots (Fig. 4A). I obtained similar findings from E15.5 and E18.5 (Fig. 4B, Fig. 4C and Fig. 5A). However, the formation of the GFP-LC3 dots was extensively induced after a natural birth. The formation of GFP-LC3 dots was upregulated within 30 min after birth (Fig. 4D). The number of GFP-LC3 dots reached its maximal level 3-6 h after birth (Fig. 4E and F and Fig. 5C), although the neonatal mice began suckling before that time. The number of dots gradually decreased to basal levels by day one or two (Fig. 4G and H).

In embryonic period, a few autophagosomes were present in other tissues, such as the diaphragm (Fig. 6A), skeletal muscle (Fig. 6C), liver (Fig. 5 M and Fig. 6E), lung (Fig. 6G), pancreas (Fig. 5E and Fig. 6I) and skin (Fig. 6K). However, the autophagosomes of these tissues were also increased after birth. Particularly, the diaphragm (Fig. 7B), skeletal muscle (Fig. 6D), liver (Fig. 5O and Fig. 6F), lung (Fig. 6H), pancreas (Fig. 5G and Fig. 6J) and skin (Fig. 6L) displayed massive dots. Autophagosomes were induced beginning 30 min after birth, and the number of dots reached its maximal level, though the degree of various level, at 3-6 h after birth (Fig. 7). The remarkable exception was thymic epithelial cells, which possessed large numbers of GFP-LC3-positive dots, even in embryos (Fig. 8A and B). The opposite phenomenon was observed in neural cells within the brain (Fig. 9A and B). These cells exhibited few or no GFP-LC3 dots in embryos.

To rule out the possibility that the LC3-positive dots represented a structure unrelated to autophagosomes, I examined GFP-LC3 localization in animals on the *Atg5^{-/-}* background (Fig. 5). As expected, the small green dots disappeared in the embryonic tissues of *Atg5^{-/-}* GFP-LC3/+ mice. These data confirmed that GFP-LC3 dots represent autophagosomes.

The appearance of autophagic vacuoles was confirmed by electron microscopy (Fig. 10A; produced by Dr. Yamamoto, Department of Bio-Science, Nagahama Institute of Bio-Science and Technology). Morphometric analysis of electron micrograph images revealed that autophagic vacuoles occupied 0.12% and 1.00% of the total cytoplasmic area in hearts isolated from neonates 0 h and 6 h after birth, respectively (Fig. 10B).

Autophagy occurs constitutively active in the thymus

In the thymic epithelial cells, autophagy was observed high basal levels from embryo to neonate (Fig. 8A and B), suggesting that autophagy was occurred independently of nutrient conditions. To study this possibility, I observed thymic epithelial cells of adult mice in nutrient rich conditions (Fig. 8C-E). GFP-LC3 dots were observed high level in stromal cells with stellate shapes in both the cortex and medulla. Because they stained with anti-cytokeratin antibody, these cells were identified as epithelial reticular cells. Small GFP-LC3 dots were present in both the cell bodies and processes of the reticular cells. It is noteworthy that autophagy in the thymic epithelial cells occurs even without starvation treatment. The number of GFP-LC3 dots was not induced in food withdrawal in these cells. Therefore, autophagy in the thymic epithelial cells is constitutively active, irrespective of nutrient conditions.

GFP-LC3 is aggregated in neonatal hepatocytes in *Atg5^{-/-}* mice

I next examined neonatal tissues of *Atg5^{-/-}* GFP-LC3/+ mice. As in the embryonic tissues, the small GFP-LC3 dots representing autophagosomes could not be detected in *Atg5^{-/-}* GFP-LC3/+ newborns. Larger, more intense fluorescent dots, however, appeared frequently in hepatocytes (1-3 dots per cell; Fig. 5P) and DRG neurons (4-8 dots per cell; Fig. 5T). While these large dots appeared occasionally in

cells of the anterior lobe of the pituitary gland (Fig. 5X), they were rarely seen in cardiac muscle or thymic epithelial cells. In the pituitary, these structures were seen as early as E15.5 (Fig. 5V). All of these structures were homogeneously fluorescent, not ring-shaped, even when quite large, suggesting that these structures are not true autophagosomes. This hypothesis is supported by the observation that LC3-II, the phosphatidylethanolamin (PE)-conjugated form of LC3, was not generated in *Atg5*^{-/-} liver or other tissues (Kuma *et al.*, 2004). Such large GFP-LC3-positive structures were not observed in pancreatic acinar cells (Fig. 5H) and skeletal muscle (data not shown) of *Atg5*^{-/-} neonates.

I hypothesized that these large fluorescent structures likely represented inclusion bodies (IBs) containing the unconjugated GFP-LC3 protein, which was not membranous structures. As intracellular IBs usually contain ubiquitin (Orth *et al.*, 2003; Watanabe *et al.*, 2001), I determined whether these structures were also positive for ubiquitin antibody. Indirect fluorescence microscopy using an anti-ubiquitin antibody showed the colocalization of GFP-LC3 and ubiquitin in *Atg5*^{-/-} hepatocytes (Fig. 11A).

The overexpression of GFP-LC3 may have caused the artificial aggregation of GFP-LC3. I thus examined the presence of IBs in the hepatocytes of wild-type and *Atg5*^{-/-} mice who did not express GFP-LC3 (Fig. 11B). While ubiquitin-positive IBs were observed in *Atg5*^{-/-} hepatocytes, these structures were absent from wild-type hepatocytes and dorsal root ganglion (DRG) neurons. Endogenous LC3 was detected in the IBs of *Atg5*^{-/-} neonate DRG neurons (Fig. 11C), suggesting that LC3 may be incorporated into protein aggregates regardless of its PE-conjugation status. The aggregation of endogenous LC3 was unclear in hepatocytes, potentially due to the lower expression of LC3 in hepatocytes. These results suggest that the absence of autophagy leads to the formation of IBs, which contain ubiquitin, in some tissues.

Accumulation of IBs in *Atg5*^{-/-} mice

Next, I determined the tissues of *Atg5*^{-/-} neonates that exhibited IB formation by immunohistochemistry using an anti-ubiquitin antibody. As observed in *Atg5*^{-/-} GFP-LC3/+ neonates, ubiquitin-positive IBs accumulated extensively in the liver (Fig.

12B), some regions of the brain (Fig. 12F), and the anterior pituitary gland (Fig. 12J) and less frequently in the heart and thymic epithelium (data not shown). In the nervous system, large aggregates were primarily observed in large neurons of the spinal cord (ventral horn cells, Fig. 12D), the pons (Fig. 12F), DRG neurons (Fig. 12H), the hypothalamus, the mid brain, and the trigeminal ganglia (data not shown). The neurons within DRG exhibited the most extensive accumulation of IBs; more than 10 aggregates were observed in a single cell slice. A subset of the IBs was as large as 2 μ m in diameter. These IBs were evenly distributed throughout the cytoplasm; they were not clustered in the perinuclear regions or around the nuclei. In contrast, neural cells in the cortex (Fig. 12L) and cerebellum (data not shown) did not contain ubiquitin-positive IBs. Other tissues, such as lung, spleen, pancreas, intestine, and skeletal muscle, also did not contain intracellular aggregates that labeled with ubiquitin (data not shown).

Immunoelectron microscopy using a gold-conjugated anti-ubiquitin antibody of DRG neurons isolated from *Atg5*^{-/-} neonates demonstrated the specific association of gold particles with amorphous intracellular structures and compact structures surrounding filamentous materials (Fig. 13A and B; produced by Dr. Yamamoto, Department of Bio-Science, Nagahama Institute of Bio-Science and Technology). As these structures were not observed in wild-type littermates, these structures may correspond to the large inclusions seen by light microscopy. These data suggest that the suppression of constitutive autophagy for only a short embryonic period is sufficient to impair protein quality control in embryonic cells, particular hepatocytes and neural cells.

Normal cell death in autophagy-deficient mice

The presence of cytoplasmic IBs prompted us to question if cell death occurred more frequently in *Atg5*^{-/-} neonates. Conventional hematoxylin and eosin staining did not reveal any significant changes in the brain or other tissues in *Atg5*^{-/-} neonates (data not shown). I determined if there was excess apoptotic cell death in *Atg5*^{-/-} newborns by TUNEL labeling. TUNEL-positive cells did not increase in *Atg5*^{-/-} tissues, even within DRG, the pons, or the hypothalamus, all sites in which ubiquitin-positive aggregates

accumulated (Fig. 14 and data not shown). These data suggest that, while the defect in autophagy during embryogenesis could accumulate IBs, it does not lead to increased cell death.

Organelle degradation in lens fiber cells occurs normally

In addition to the clearance of abnormal intracellular proteins, autophagy is required for the degradation of normal proteins and organelles in a subset of specialized cells, such as lens and erythroid cells. Next, I examined a possible role of autophagy in organelle degradation during lens differentiation. The lens contains only two types of cells, the epithelial cells covering the anterior surface of the lens and the fiber cells that differentiate from the epithelial cells. During differentiation, entire organelles within the epithelial cells are lost, which allows fiber cells to be transparent. Similarly, intracellular organelles are eliminated during erythroid cell maturation. Several studies have suggested the involvement of autophagy in these processes. Since the organelle free zone (OFZ) in the lens is created between 17.5 days post conception (dpc) and birth, I first determined the occurrence of autophagy at this stage by using of GFP-LC3 transgenic mice (Fig. 15B and C). In lens of 17.5 dpc embryos, a number of GFP-LC3 dots were observed at the center region. Fewer GFP-LC3 dots were observed at the border of developing OFZ. To rule out the possibility that these LC3-positive dots represented structures unrelated to autophagosomes, I examined GFP-LC3 localization in lens at the same stage on the *Atg5*^{-/-} background (Fig. 15E and F). As expected, these small green dots were not detected in the lens epithelial cells of GFP-LC3 *Atg5*^{-/-} mice. These data confirmed that autophagy occurred continuously in embryonic lens, particularly at the center region.

To determine whether autophagy is involved in organelle degradation, I examined the existence of organelle in lens by immunohistochemical analysis during embryogenesis. At lens of 17.5 dpc wild-type (*Atg5*^{+/+}) embryos, nuclei and endoplasmic reticulum (ER), stained with Hoechst 33258 and anti-KDEL antibody, respectively, were present abundantly (Fig. 16A). Both the ER and the nuclei at the center region of the lens disappeared after birth, and OFZ was created. At day 0.5

neonates, no ER and only a small amount of nuclear debris could be observed in the OFZ (Fig. 16C). I next analyzed this rapid process under autophagy-deficient conditions using *Atg5^{-/-}* mice. At 17.5 dpc, lens of normal size and morphology were generated in the mutant mice (Fig. 16B), suggesting that autophagy is not required for lens morphogenesis from the optic primordial. In addition, OFZ was created at day 0.5 neonates in *Atg5^{-/-}* mice in a manner similar to that in wild-type mice (Fig. 16D). I prolonged the survival of neonates by artificial feeding and analyzed the OFZ formation up to 2 days after birth, but there was no significant difference between *Atg5^{+/+}* and *Atg5^{-/-}* mice (Fig. 16E and F).

The generation of normal lens fibers was confirmed by electron microscopy. The cytoplasm of lens fibers in OFZ of both *Atg5^{+/+}* and *Atg5^{-/-}* consisted of fine granular crystalline substance, where organelles were not observed. These data suggest that autophagy is dispensable for OFZ formation in the lens.

Discussion

Induction of autophagy in neonatal period

In this study I examined autophagy kinetics in embryonic and prenatal stage, and observed that autophagy remained at a low level throughout the embryonic period. However, the formation of the autophagosomes was extensively induced in various tissues after a natural birth (Fig. 4, Fig. 6 and Fig. 7). Such an induction pattern is different from that of starved adult mice. This might be because the energy requirements of the heart and diaphragm suddenly increase at birth, and the external environments of lung and skin are drastically changed; that is, from the amniotic fluid to the air. The plasma amino acid concentration was measured under fasting condition, because the major role of autophagy is the degradation of proteins into amino acids (Kuma *et al.*, 2004). Soon after caesarean section, the concentration of amino acid in the plasma of *Atg5^{-/-}* neonates was not different from that of wild-type littermates. However, at 10 h after the caesarean delivery, the total amino acid concentration of *Atg5^{-/-}* mice was significantly lower than that of wild-type mice. In the organs, such as heart, liver and brain, the total amino acid concentration did not differ significantly among littermates at birth. However, after 10 h, significant differences were observed in those organs. Mammals encounter the first, and probably the most severe, period of starvation during their lifespan in soon after birth by the sudden termination of the trans-placental nutrient supply. To overcome this life-threatening problem unique to mammals, it has been known that carbohydrate and lipid reserves are used during period. In addition, autophagy must be activated to maintain an adequate amino acid pool until the nutrient supply from milk reaches a steady state. Amino acids produced by autophagy can be directly used as an energy source or converted to glucose in the liver. Alternatively, amino acids can also be used for synthesis of proteins required for the proper starvation response. Considering that the developmental defects of autophagy mutants reported in other species are related to nutrient starvation, it is thought that mammalian autophagy play very important role also for neonatal survival (Fig. 17).

Constitutively active autophagy in the thymic epithelial cells

Several tissues, including thymic epithelial cells (Fig. 8) and some exocrine gland cells such as pituitary gland cells (Fig. 5) showed high basal levels of autophagy from embryo to neonates. Although the volume of thymic epithelial cells is difficult to estimate by fluorescence microscopy, the number of autophagosomes in these cells might be the highest of any nonstarved tissue. One report has also demonstrated the extensive acid phosphatase activity in some vacuoles in the thymic epithelial cells (Bowen and Lewis, 1980). Younger mice (8 weeks old) and late-stage embryos (15.5-19.5 dpc embryo) show more active autophagy in the thymus. In general, cytoplasmic proteins are processed by the proteasome, delivered into the lumen of the ER and presented by the MHC class I pathway. However, there is a growing amount of data demonstrating that endogenous proteins are also presented on MHC class II (Lechler *et al.*, 1996). How cytoplasmic proteins are loaded on MHC class II has not been well studied, but autophagy is likely responsible for this pathway (Paludan *et al.*, 2005; Dengjel *et al.*, 2005; Nimmerjahn *et al.*, 2003). During positive and negative selections, thymic epithelial cells present self-antigens to lymphocytes. Because thymic epithelial cells are not thought to have phagocytic activity, it is reasonable to hypothesize that they provide self-antigens from their own cytoplasm. In this scenario, autophagy might be involved in T-cell development and central tolerance in thymic epithelial cells.

Intracellular clearance by constitutive autophagy

In this study, I have described the role of autophagy in mammalian embryo and neonates. As yeast cells defective in autophagy do not exhibit obvious abnormalities until cultured under nutrient medium condition (Takeshige *et al.*, 1992), the role of basal level autophagy has been ignored. In a similar manner, autophagy-deficient mammalian cells, such as *Atg5*^{-/-} embryonic stem cells (Mizushima *et al.*, 2001) and embryonic fibroblasts (Kuma *et al.*, 2004), also do not exhibit significant abnormalities, despite low level of constitutive autophagy in the wild-type parental cells. As these cells can divide rapidly, abnormal proteins would be quickly diluted and would not

accumulate, even if not degraded. Thus, the importance of basal autophagy likely depends on cellular context. In this study, I demonstrated that requirement for autophagy differs between embryonic tissues. Extensive IB (inclusion body) formation was detected only in a few tissues, including neural cells, hepatocytes, and anterior pituitary gland cells (Fig. 12). Recently, basal autophagy was demonstrated to be important for liver homeostasis using mice bearing a tissue-specific deficiency of Atg7 (Komatsu *et al.*, 2005). I demonstrated that a deficiency of autophagy over a much shorter time, from liver genesis to birth, sufficient to generate large inclusions in hepatocytes; these ubiquitin-positive aggregates were already present in a subset of hepatocytes at E15.5 in *Atg5^{-/-}* embryos. In addition, I revealed that neural cells and anterior pituitary cells are additional cell types in which protein quality control is highly dependent on basal levels of autophagy (Fig. 17).

The reason that autophagy is particularly important in these cells remains unclear. The basal levels of autophagy may be particularly high in these tissues. DRG neurons and anterior pituitary gland cells do exhibit higher levels of autophagy than other tissues (Fig. 5). The basal level of autophagy, however, does not always correlate with the degree of IB formation in *Atg5^{-/-}* tissues. Thymic epithelial cells exhibit the most extensive autophagy seen throughout embryos, but only a few IBs are generated in this tissue in autophagy-deficient animals (Fig. 5). In contrast, while autophagosomes are not observed in regions of the central nervous system, such as the hypothalamus and pons, in wild-type mice, IBs accumulate in these tissues in *Atg5^{-/-}* mice. The time needed to reach the postmitotic state may also influence the dependence of individual tissues on autophagy. The longer the time period that passes after cells stop dividing, the more abnormal proteins could accumulate within a cell. The lack of significant numbers of IBs in cortical neurons may be due to the young developmental age of these cells in comparison to neurons within sensory roots. In addition, cell types may differ in their expression of proteins that easily aggregate or whose quality is tightly regulated. Further detailed analysis of the protein composition of these aggregates may be needed to address this possibility.

Mechanism of Ub-positive aggregate formation

The mechanism governing the accumulation of ubiquitin-positive aggregates in *Atg5^{-/-}* tissues is not clear. Autophagy is thought to be a non-selective process. The turnover of long-lived proteins is impaired under autophagy-defective conditions (Komatsu *et al.*, 2005), which would make these proteins more prone to damaged or misfolding. Under these conditions, these proteins would have an increased chance of being both ubiquitinated and aggregated. This scenario does not imply any selectivity of autophagy. In autophagy-competent cells, microaggregates could also be sequestered into autophagosomes by chance.

Recently, selective or preferential sequestration/degradation of cytosolic contents by autophagy was reported. In yeast, the Ald6 protein was degraded in an autophagy-dependent manner more rapidly than other cytosolic proteins (Onodera *et al.*, 2004). Although it remains unknown if a similar preferential degradation of cytosolic contents occurs by autophagy in mammals, invading bacteria that enter into the cytosol seem to be selectively enclosed (Nakagawa *et al.*, 2004; Ogawa *et al.*, 2005). Proteins on the inner face of autophagosomal membranes may participate in the specific recognition of a subset of molecules. During the autophagic degradation of intracellular *Shigella* species, the bacterial VirG protein may be recognized by autophagic membranes (Ogawa *et al.*, 2005). This kind of substrate recognition is observed in an autophagy-related system in yeast. Two vacuolar proteins, aminopeptidase I and α -mannosidase, are selectively transported to vacuoles by the CVT pathway. Under nutrient-rich conditions, this process is mediated by an autophagosome-like structure called a Cvt vesicle (Klionsky, 2005). During starvation, these two enzymes are delivered to the vacuole by autophagosomes. A common receptor (Atg19) for these proteins is present on both types of sequestration membranes. Although no equivalent pathway has been discovered in other species, this process may be the prototype of selective sequestration. As a number of studies have suggested the selective delivery of ubiquitinated proteins to lysosomes (Schwartz *et al.*, 1988; Doherty *et al.*, 1989; Laszlo *et al.*, 1990; Ueno and Kominami, 1991; Lenk *et al.*, 1999), ubiquitinated or misfolded

proteins may also be recognized by as-yet unknown proteins on autophagic membranes.

Another, but not mutually exclusive, possibility is that autophagy selectively, via p62, eliminates IBs that have already formed (Bjorkoy *et al.*, 2005). I have not, however, observed such a selective enclosure of large IBs in wild-type cells. On the other hand, autophagosome is recruited to IBs via microtubules (Iwata *et al.*, 2005). Although several studies demonstrated the co-localization of LC3 and IBs, this phenomenon may reflect the incorporation of LC3 into IBs, rather than autophagosome sequestration (Fig. 11C). In addition, because IBs are usually larger than typical autophagosomes (about 1 μm), it is unlikely that autophagosomes enclose inclusions of this size efficiently. I cannot, however, rule out the possibility that small aggregates are preferentially sequestered into autophagosomes.

Relevance to pathophysiology of neurodegeneration

I demonstrated that the neural cells of *Atg5^{-/-}* mice exhibit morphological alterations (accumulation of IBs). The presence of multiple inclusions in certain types of neurons in *Atg5^{-/-}* mice suggests that soluble abnormal proteins accumulate due to a general impairment in protein turnover. A recent study indicated that the soluble forms of mutant proteins, rather than the aggregated forms, are the major cause of toxicity for neurons (Saudou *et al.*, 1998; Taylor *et al.*, 2003; Arrasate *et al.*, 2004). Therefore, the contribution of autophagy to neuronal homeostasis could be much greater than that perceived from the presence of intracellular inclusions.

The ubiquitin-proteasome system is considered to be the primary means for degradation of misfolded proteins. This study, however, indicates that autophagy collaborates with this process to prevent the accumulation of abnormal proteins. This finding has implications in the pathophysiology of neurodegenerative disease. Multiple studies have suggested that the inhibition of autophagy induces the aggregation of mutant proteins that are detected in human diseases; rapamycin-induced upregulation of autophagy reduces this aggregate formation (Teckman *et al.*, 2000; Ravikumar *et al.*, 2002; Fortun, 2003; Ravikumar and Rubinsztein, 2004). This study demonstrates that inhibition of autophagy causes aggregation, even in the absence of mutant protein

expression.

Organelle degradation in lens fiber cells

Intracellular organelles are lost during the differentiation of lens fiber cells and erythrocytes. The mechanism by which these organelles are destroyed during this process is not fully understood. The presence of autophagic vacuoles in these cells during differentiation suggested the involvement of autophagy in organelle degradation (Tooze and Davies, 1965; Kent *et al.*, 1966; Walton and McAvoy, 1984; Heynen *et al.*, 1985; Takano-Ohmuro *et al.*, 2000). Recently, the degradation of lens nuclei was reported to depend on DNase II-like acid DNase / DNase II β (Nishimoto *et al.*, 2003), suggesting that chromatin degradation occurs in an acidic organelle. I demonstrated that autophagy is not essential for either lens OZF formation or organelle elimination, at least before birth (Fig. 16). I do not know if further lens maturation occurs normally, because of the early lethality of *Atg5*^{-/-} mice. This data suggest, however, that an autophagy-independent mechanism of OFZ formation must exist. 15-lipoxygenase was suggested to participate in organelle degradation in lens cells by permeabilization of the organelle membranes (van Leyen *et al.*, 1998). This enzyme is highly expressed in sites at which lens organelles are degraded. The ubiquitin-proteasome system may also be involved in this form of organelle degradation (David and Shearer, 1989). Thus, I demonstrated that the degradation of nuclei in lens fiber cells is independent of autophagy. This is reasonable, because nuclei are too large to be enclosed by typical autophagosomes.

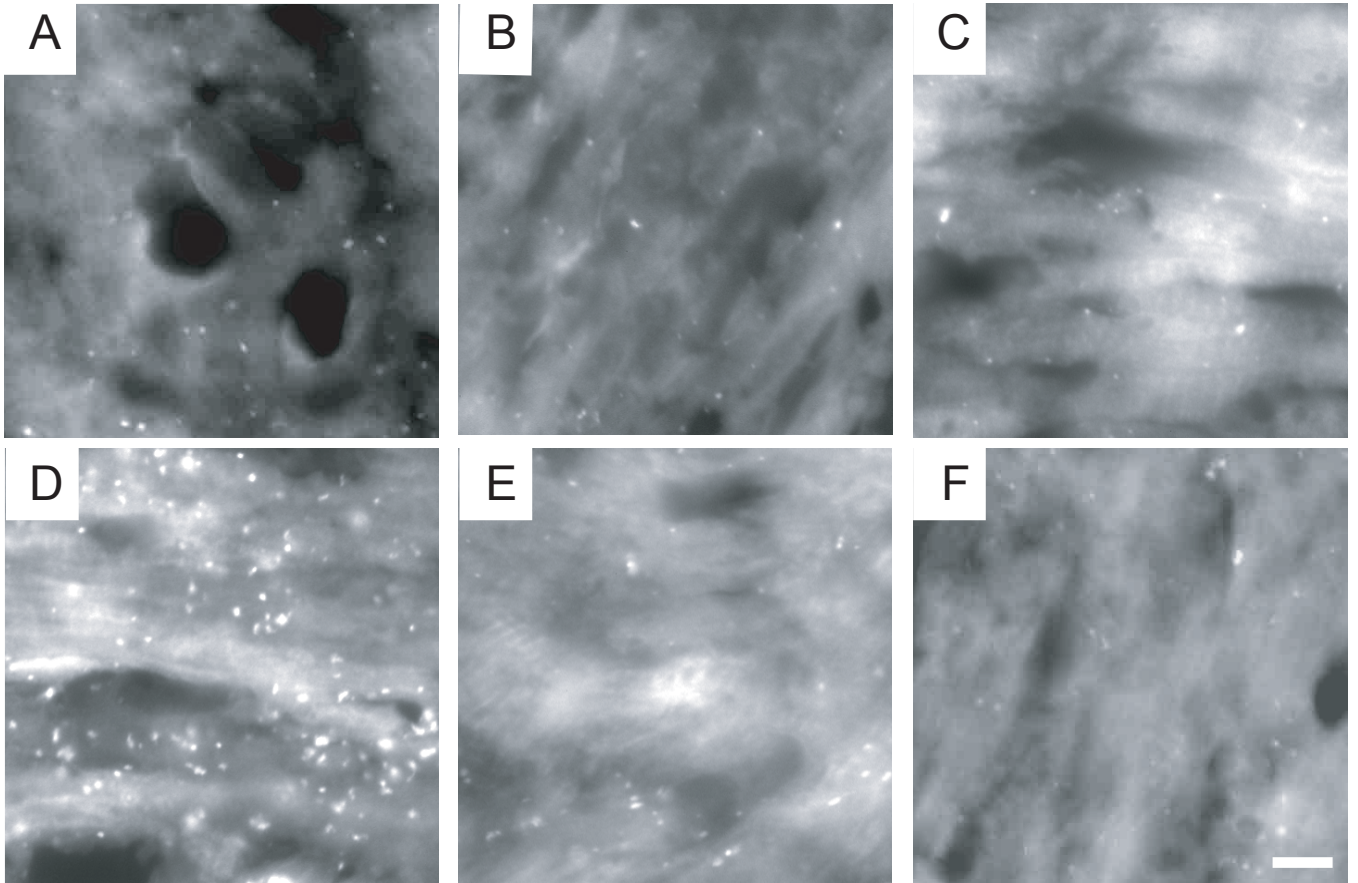


Figure 4. Localization of GFP-LC3 in the heart of embryos and neonates mice

Hearts were isolated from GFP-LC3 transgenic mice at multiple stages, including at embryonic day (A) 13.5, (B) 15.5, (C) 18.5 and (D) neonatal day 3-h, (E) 24 h and (F) 2.5 day, immediately fixed, cryosectioned, and analyzed by fluorescence microscopy. Bar, 10 μ m.

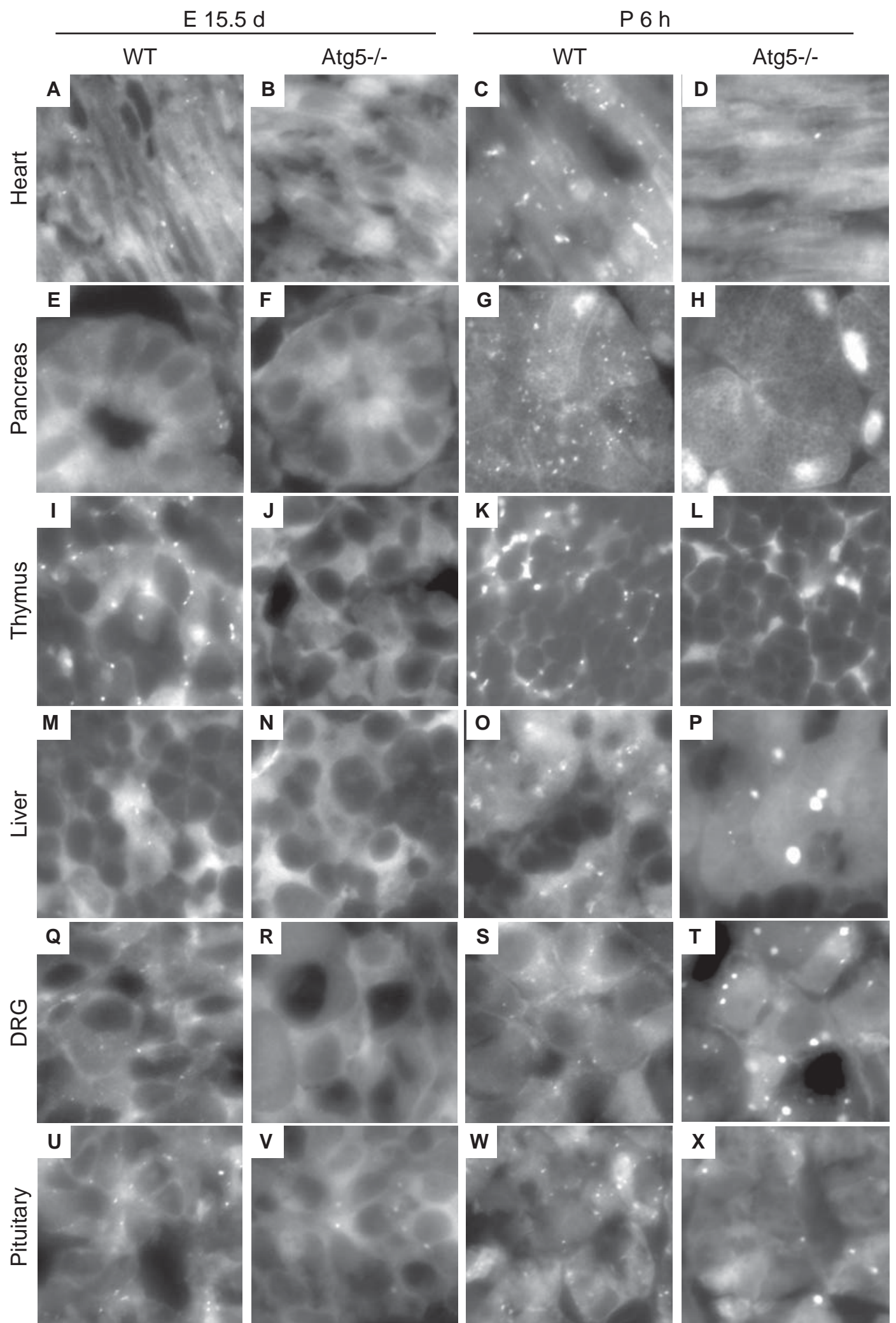


Figure 5. Localization of GFP-LC3 in various tissues of embryos and neonates

Various organs were isolated from embryonic day 15.5 embryo and 6-h neonates of heterozygous GFP-LC3 transgenic mice on the Atg5^{+/+} or Atg5^{-/-} backgrounds. Tissues were immediately fixed, sectioned, and analyzed by fluorescence microscopy. (A-D) Heart, (E-H) exocrine pancreas, (I-L) thymus, (M-P) liver, (Q-T) dorsal root ganglia, (U-X) anterior lobe of pituitary gland. (A, E, I, M, Q and U) embryonic day 15.5 embryos of Atg5^{+/+} GFP-LC3^{+/+} mice, (B, F, J, N, R and V) embryonic day 15.5 embryos of Atg5^{-/-} GFP-LC3^{+/+}, (C, G, K, O, S and W) 6-h neonates of Atg5^{+/+} GFP-LC3^{+/+} mice, and (D, H, L, P, T and X) 6-h neonates of Atg5^{-/-} GFP-LC3^{+/+} mice. Bar, 10 μ m.

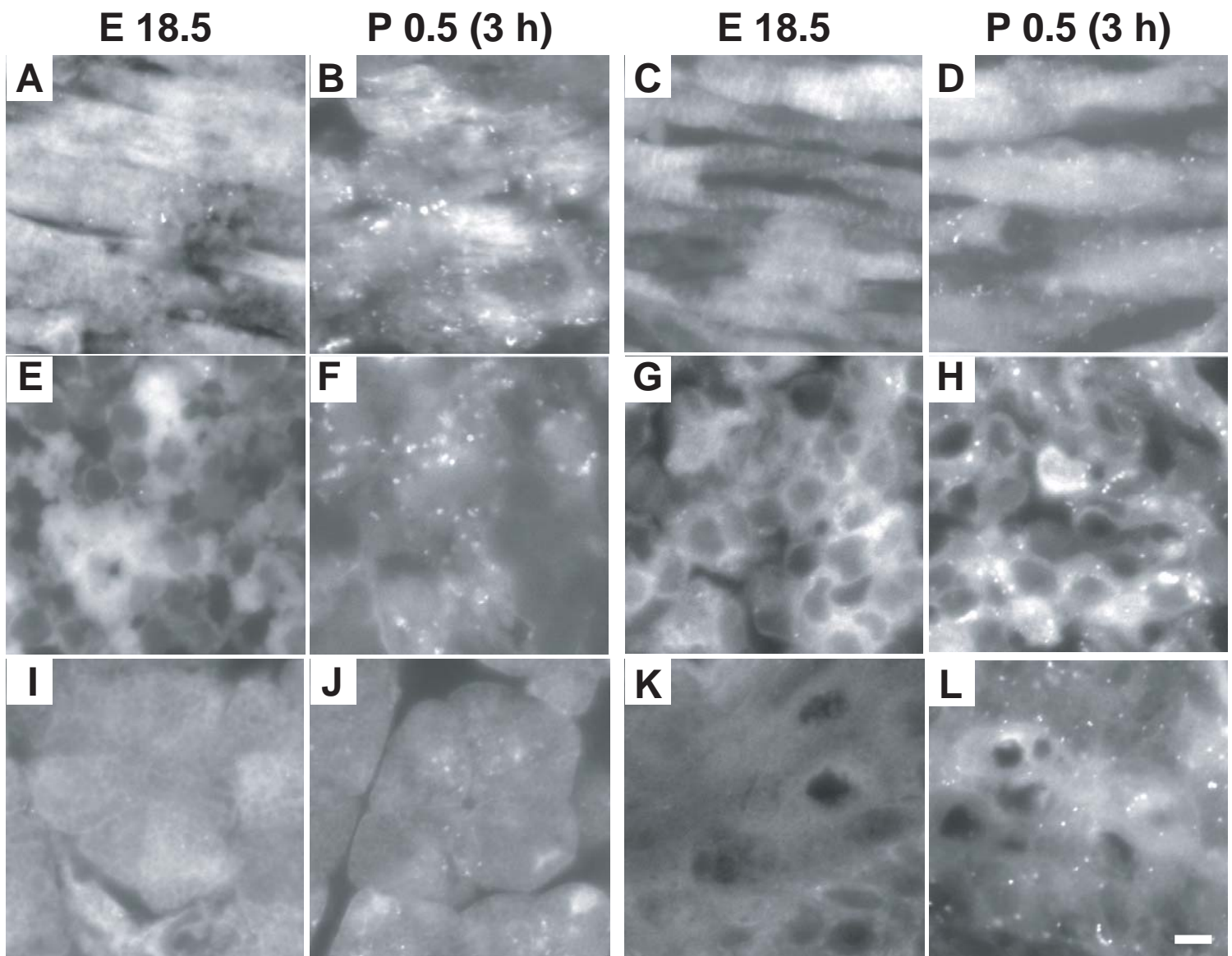


Figure 6. Autophagy is induced in various neonatal tissues

Detection of autophagy in (A and B) diaphragm, (C and D) skeletal muscle, (E and F) liver, (G and H) lung, (I and J) pancreas and (K and L) skin. These tissues were isolated from GFP-LC3 transgenic mice at embryonic day 18.5 (A, C and E) and 3 h after birth (D, D and F), immediately fixed, cryosectioned, and analysed by fluorescent microscopy. Bar, 10 μ m.

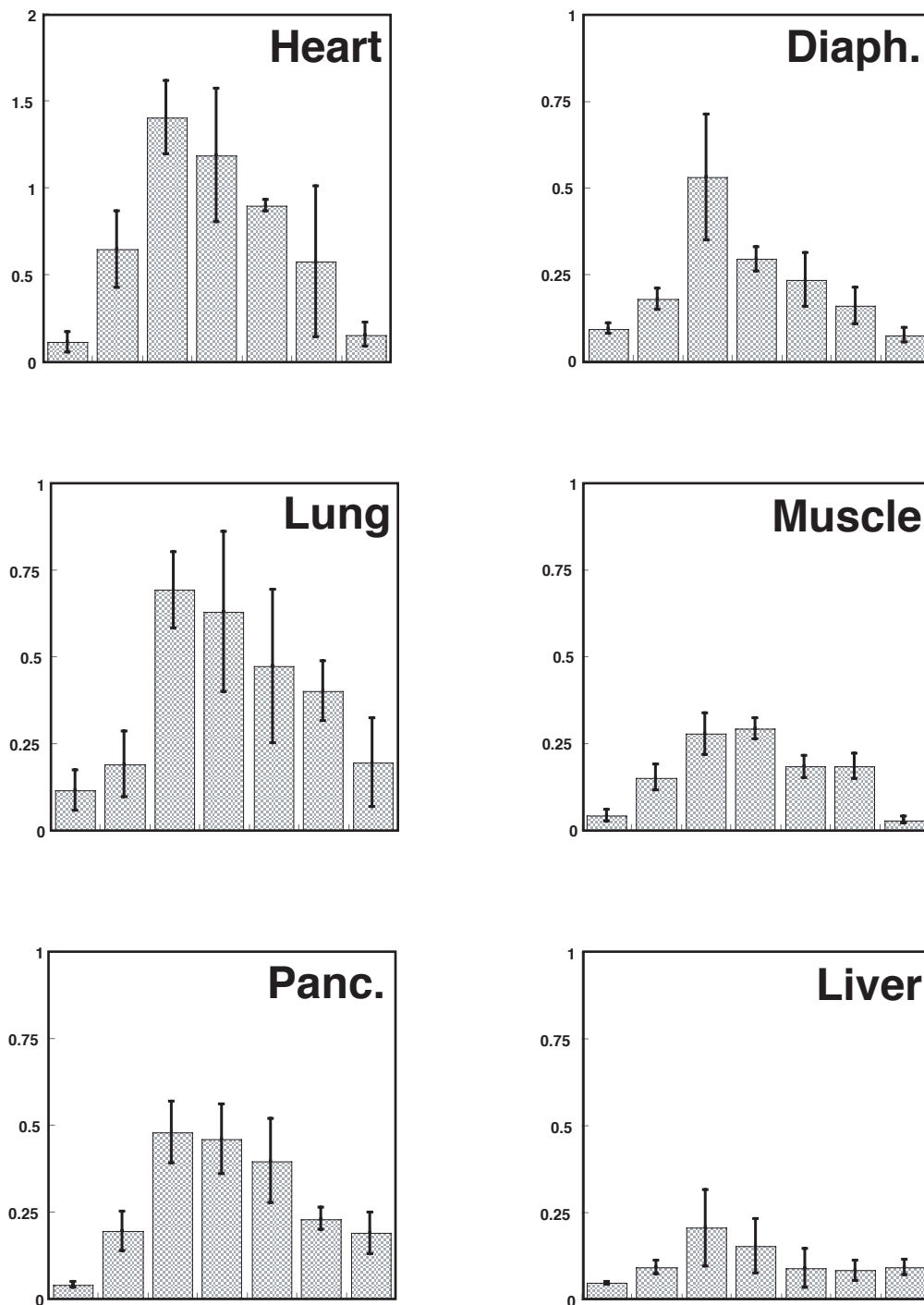


Figure 7. Quantification of GFP-LC3 dots in neonatal tissues

Cryosections were prepared from tissues isolated at the indicated times. The ratio of the total area of GFP-LC3 dots to the total cellular area is shown percentage. Values represent mean \pm s.d. of three mice. Diaph., diaphragm; Panc., pancreas; Muscle; gastronemius muscle.

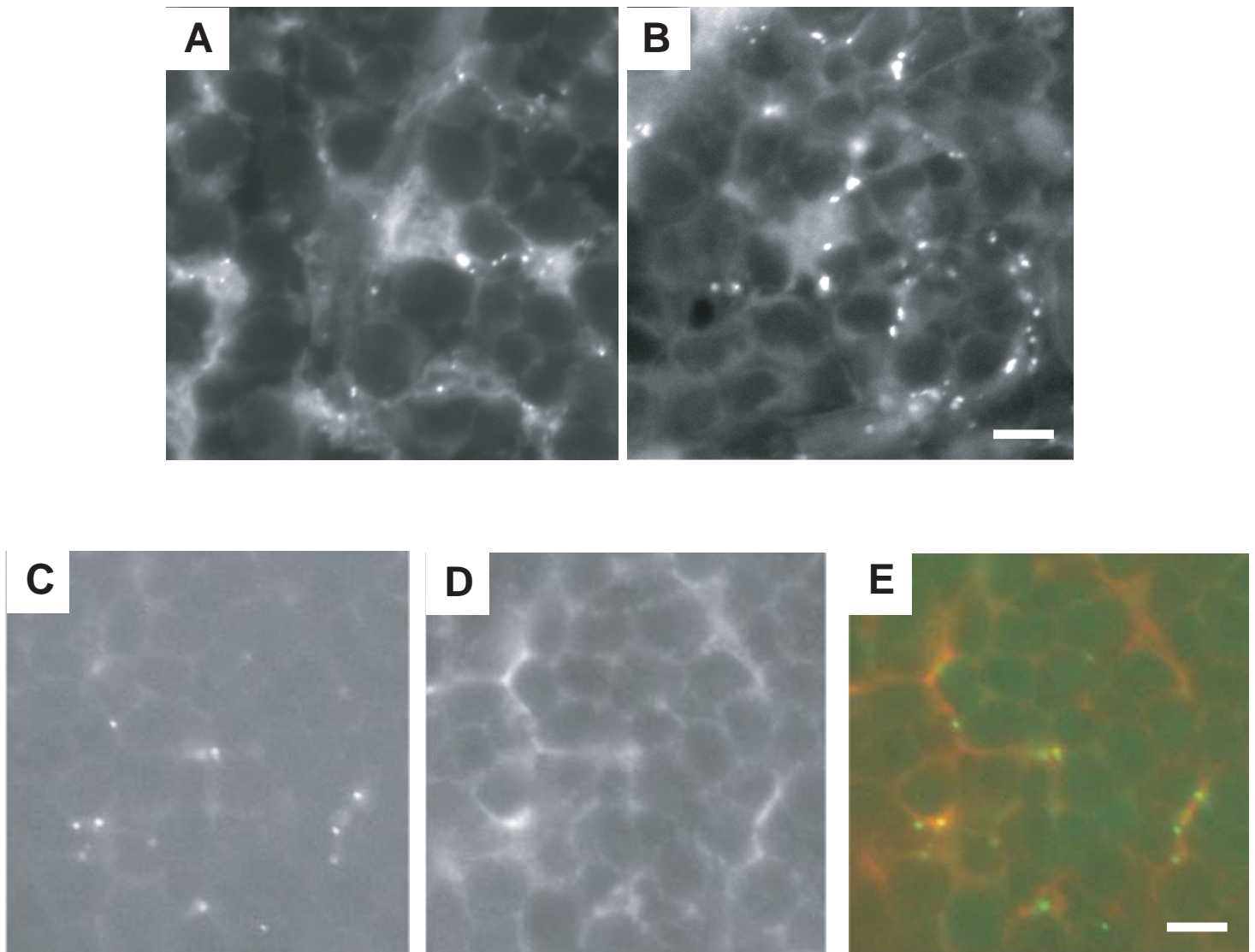


Figure 8. Localization of GFP-LC3 in the thymus of embryos and adults

Autophagosome formation in the thymus by GFP-LC3. Thymus were isolated from GFP-LC3 transgenic mice at multiple stages, including at (A) embryonic day 15.5 embryos, (B) 3-h after birth neonates and (C-E) feeding adult mice. (C) GFP-LC3 fluorescence, (D) anti-cytokeratin antibody staining and (E) merged image are shown. Bar, 10 μ m.

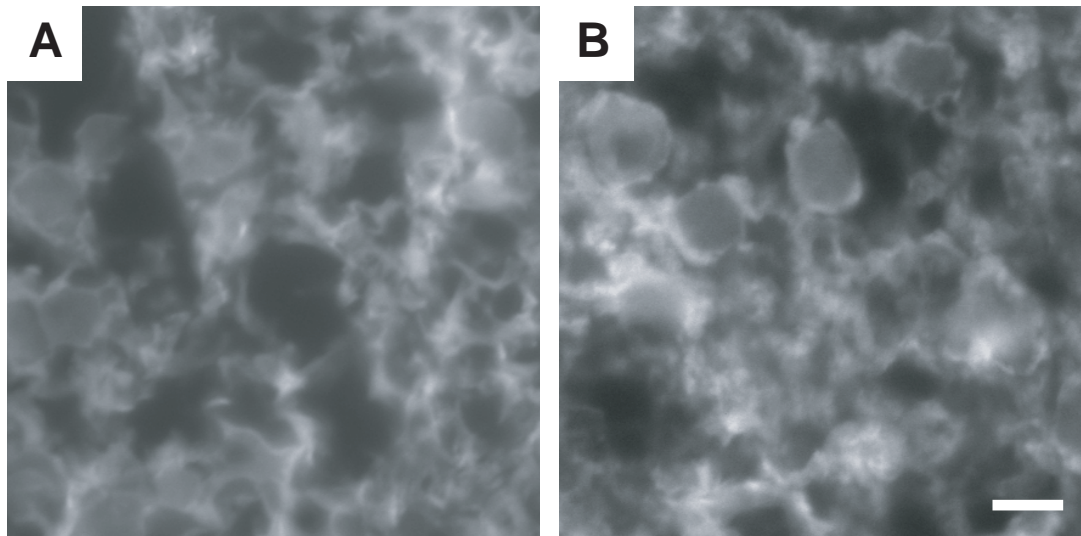


Figure 9. Localization of GFP-LC3 in the brain of embryos and neonates

Brain were isolated from GFP-LC3 transgenic mice at (A) embryonic day 15.5 embryos and (B) 3-h after birth neonates, and immediately fixed, cryosectioned, and analyzed by fluorescence microscopy. Bar, 10 μ m.

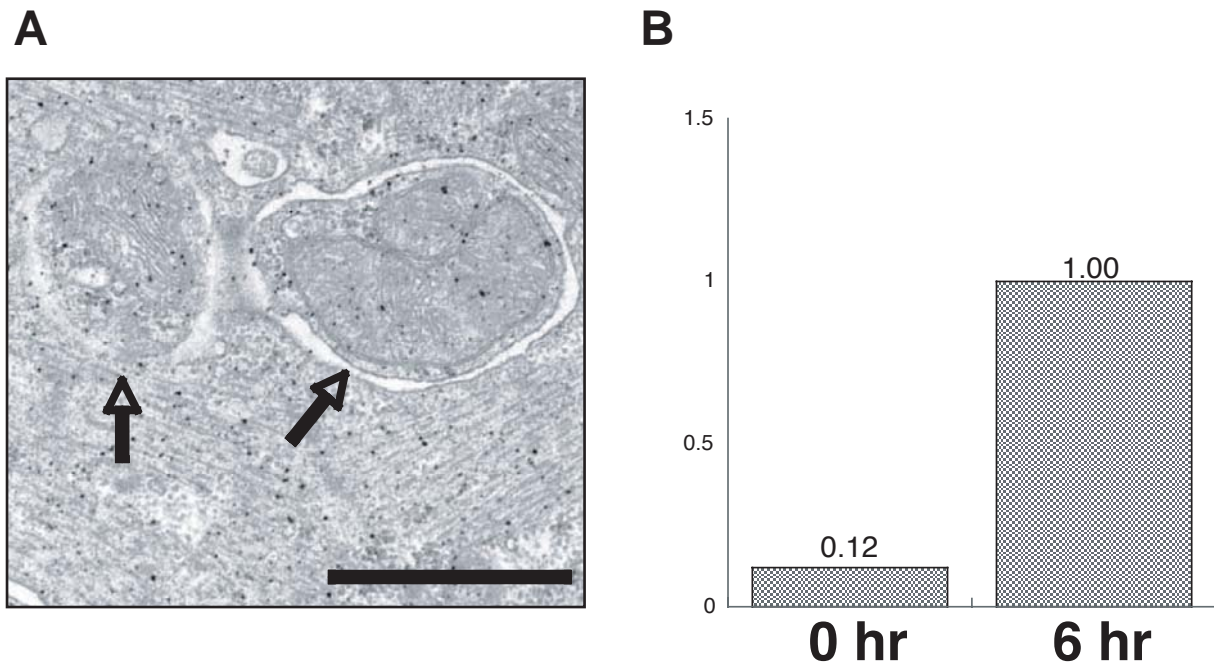


Figure 10. Electron microscopic analysis of the hearts from wild-type neonates

(A) Typical autophagosomes (arrows) were observed in the heart at 10 h after birth. Bar, 1 μ m.

(Produced by Dr. Yamamoto, Department of Bio-Science, Nagahama Institute of Bio-Science and Technology) (B) Autophagosomes were quantitated by electron microscopy and morphometric analysis. The ratio of the total area of autophagic vacuoles to the total cytoplasmic area is shown.

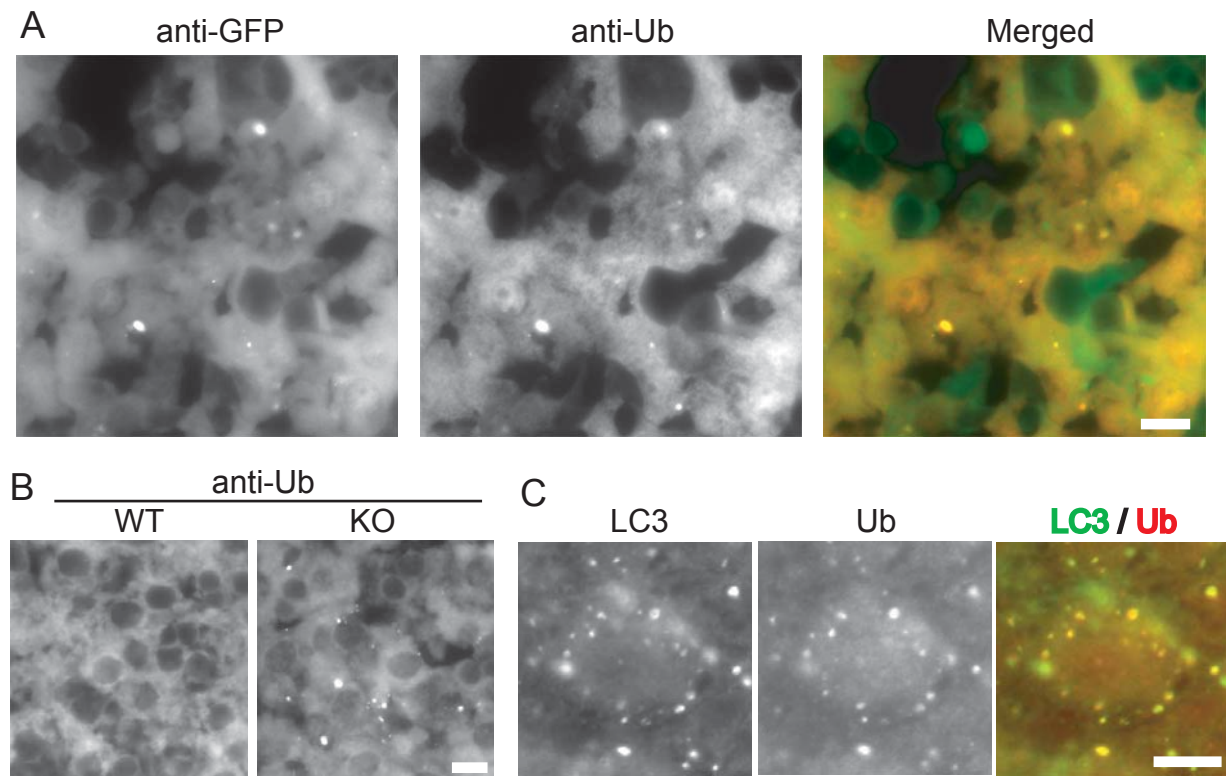


Figure 11. LC3 dot structures in *Atg5*^{-/-} represent IBs

Neonatal liver from *Atg5*^{-/-} GFP-LC3/+ (A) and *Atg5*^{-/-} (without GFP-LC3 expression) mice (B) and dorsal root ganglion from *Atg5*^{-/-} (without GFP-LC3 expression) mice (C) were examined by immunohistochemistry. OCT-embedded (A and B) and paraffin-embedded (C) sections were antigen-retrieved and stained with anti-GFP antibody (A, left), anti-ubiquitin antibody (A, middle) (B) (C, left). Merged images are shown (A, right) (C, right). Bar, 10 μ m.

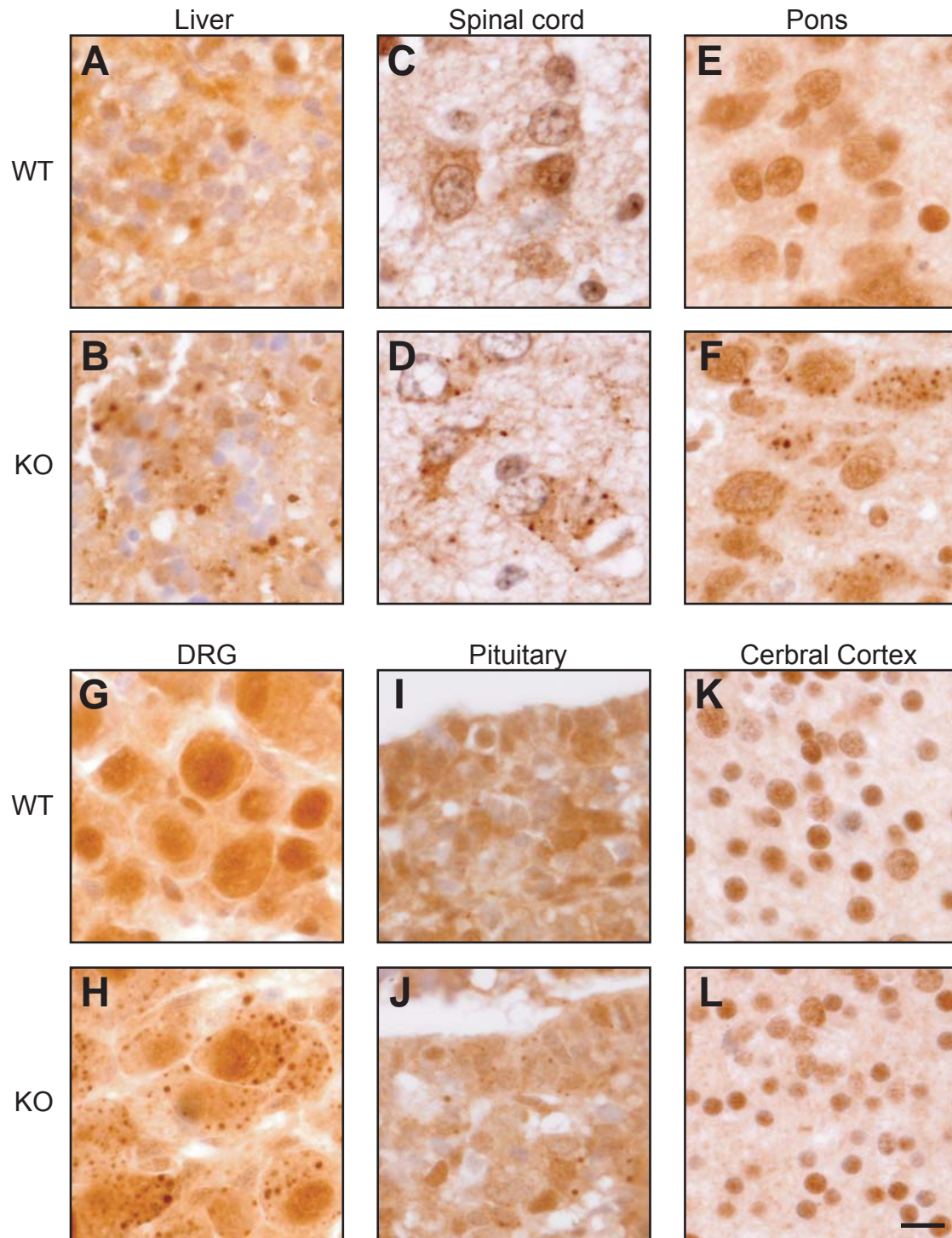


Figure 12. Ubiquitin-positive IBs accumulate in *Atg5*^{-/-} tissues

0-h neonatal tissues were fixed and decalcified. Whole mount paraffin sections of *Atg5*^{+/+} (A, C, E, G, I and K) and *Atg5*^{-/-} (B, D, F, H, J and L) neonates were prepared and stained with an anti-ubiquitin antibody. (A and B) Liver, (C and D) anterior horn of the spinal cord, (E and F) pons, (G and H) dorsal root ganglia, (I and J) anterior lobe of pituitary gland and (K and L) cerebral cortex. Bar, 10 μ m.

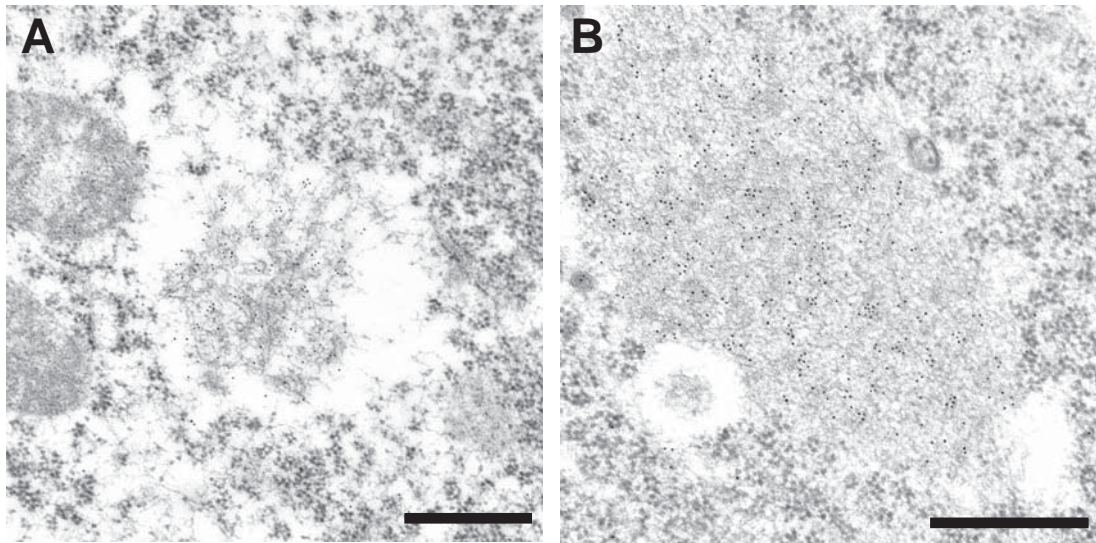


Figure 13. Immunoelectron micrograph of ubiquitin-positive IBs

DRG neurons isolated from Atg5^{-/-} neonates were analyzed by immunoelectron microscopy using a gold-conjugated anti-ubiquitin antibody. (Produced by Dr. Yamamoto, Department of Bio-Science, Nagahama Institute of BiO-Science and Technology) Gold particles were associated with (A) amorphous intracellular structures and (B) compact structures surrounding filamentous materials. Bar, 500 nm.

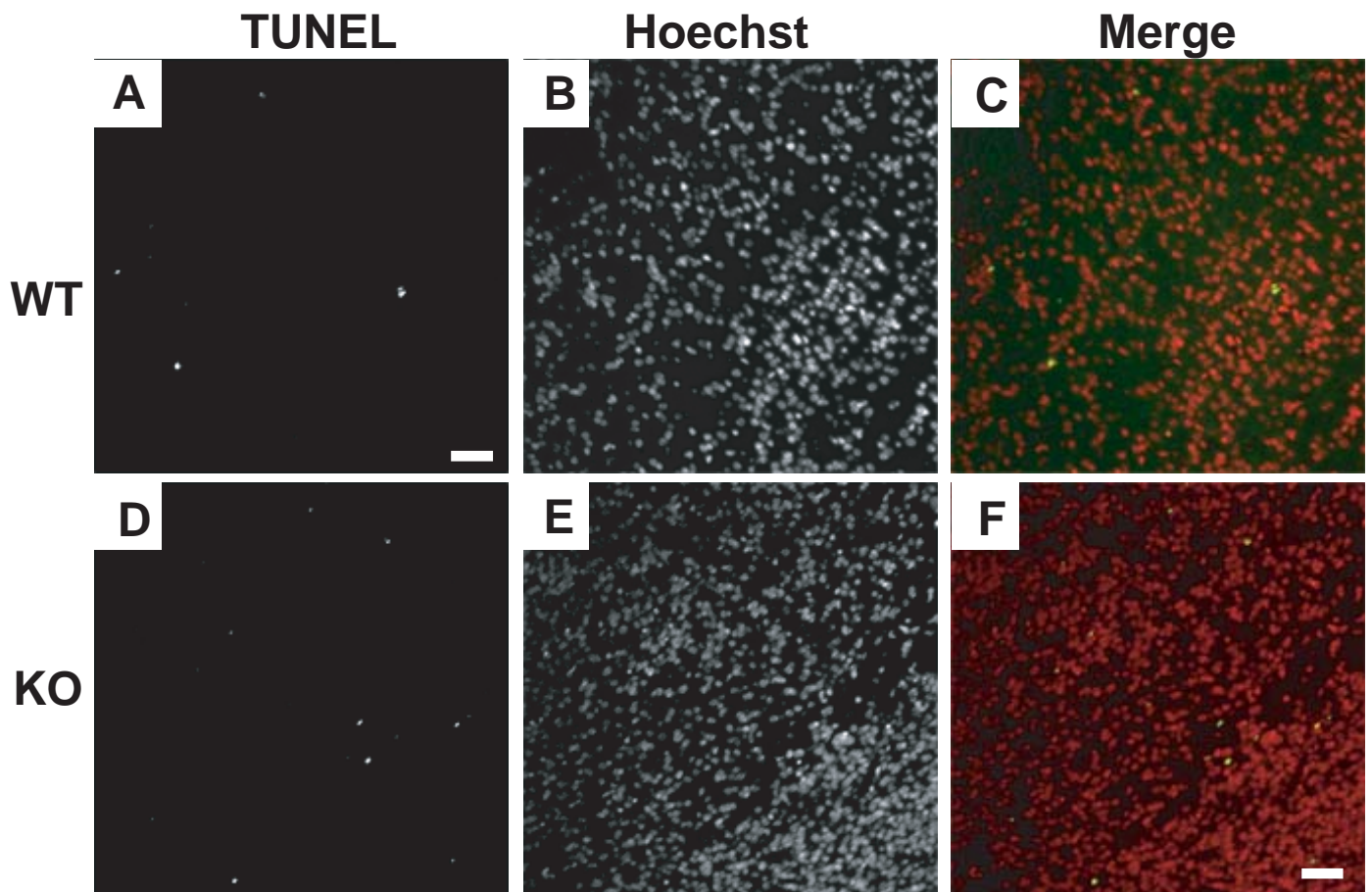


Figure 14. Normal cell death in autophagy-deficient mice

Brain was isolated from *Atg5*^{-/-} mice at postnatal day 0, and samples were fixed with 4%PFA. Cell death was detected by TUNEL method. (A-F) hypothalamus. (A-C) *Atg5*^{+/+}, (D-F) *Atg5*^{-/-} mice. Nuclei were stained with Hoechst 33258 (shown in red). Bar, 50 μ m.

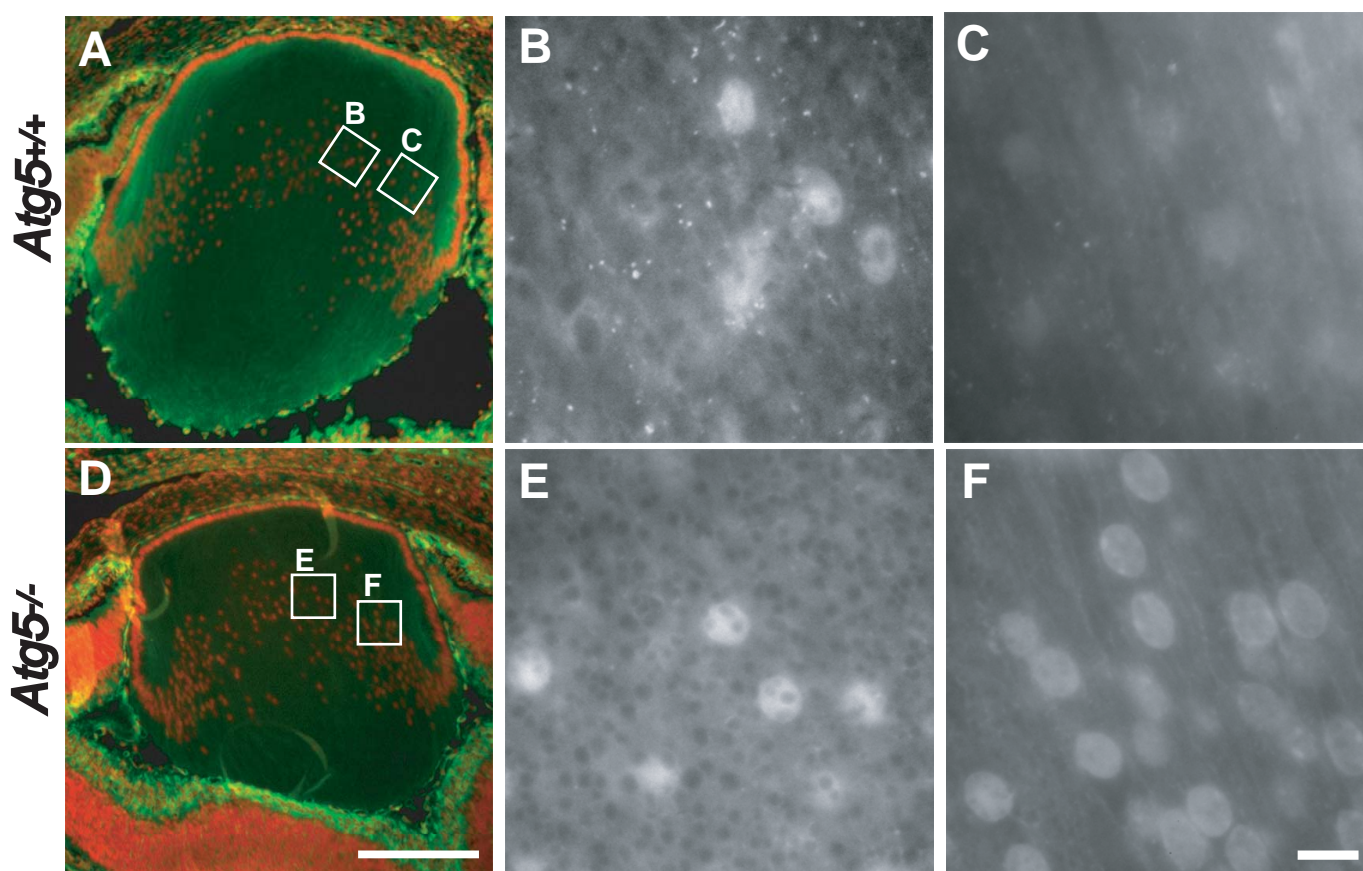


Figure 15. Localization of GFP-LC3 in embryonic lens

Lens were isolated from embryonic day 17.5 embryo of heterozygous GFP-LC3 transgenic mice on the *Atg5*^{+/+} (A-C) or *Atg5*^{-/-} (D-F) backgrounds. Lens were immediately fixed and sectioned. Nuclei were stained with Hoechst 33258 (shown in red in A and D) and analyzed by fluorescence microscopy. (B, C, E and F) Higher magnification images of GFP signals regions in (A and D). Bar, 100 μ m (A and D) and 10 μ m (B, C, E and F).

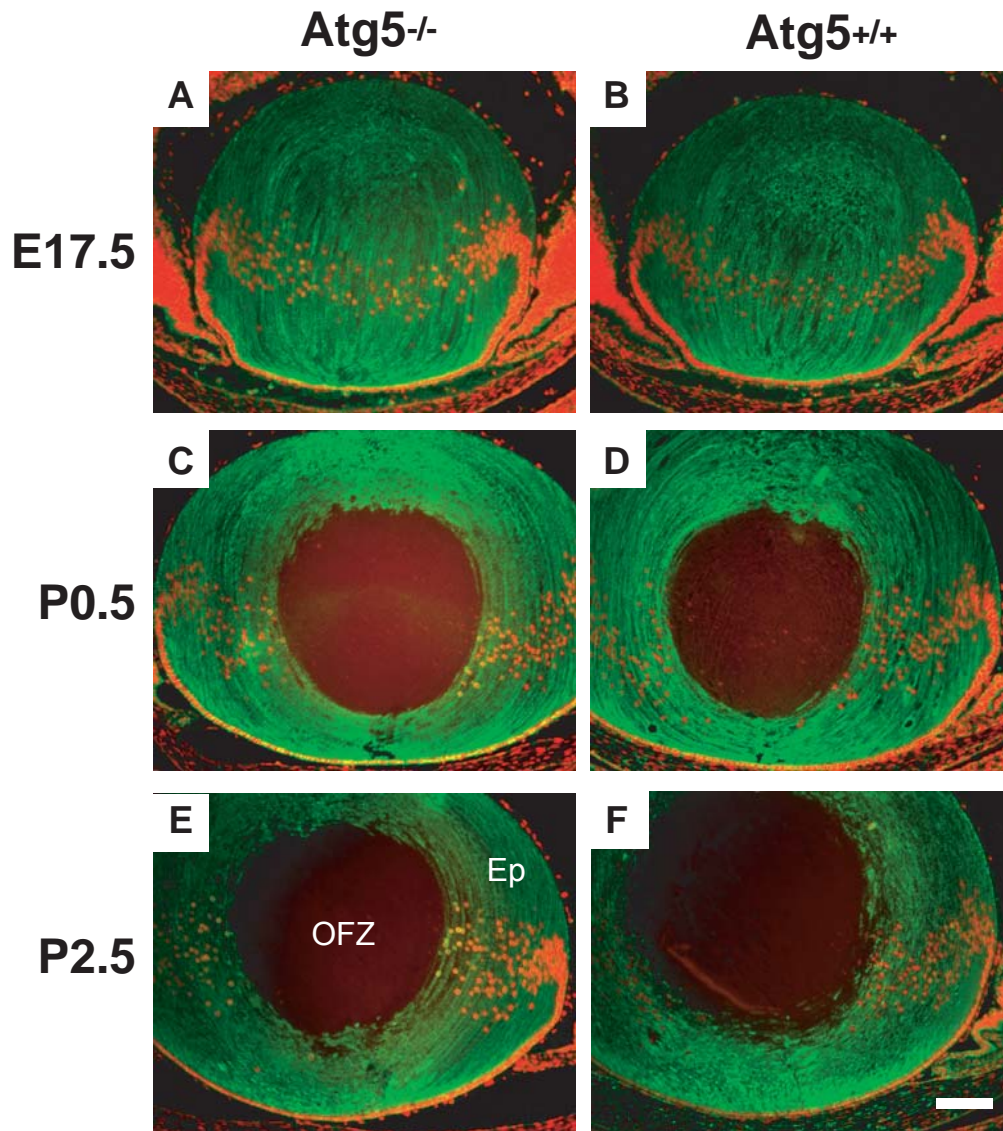


Figure 16. Normal OFZ formation in lens of *Atg5*^{-/-} mice

Mid sagittal lens slices were prepared from embryonic day 17.5 embryo (A and B) and day 0.5 neonates (C and D) and day 2.5 neonates (E and F) of *Atg5*^{+/+} (A, C and E) and *Atg5*^{-/-} (B, D and F) mice. The endoplasmic reticulum was visualized by immunostaining using an anti-KDEL antibody combined with an AlexaFluor 488-conjugated goat anti-rabbit IgG antibody (shown in green). Nuclei were stained with Hoechst 33258 (shown in red). Superimposed images are shown. Ep, epithelium; OFZ, organelle-free zone. Bar, 100 μ m.

Autophagy

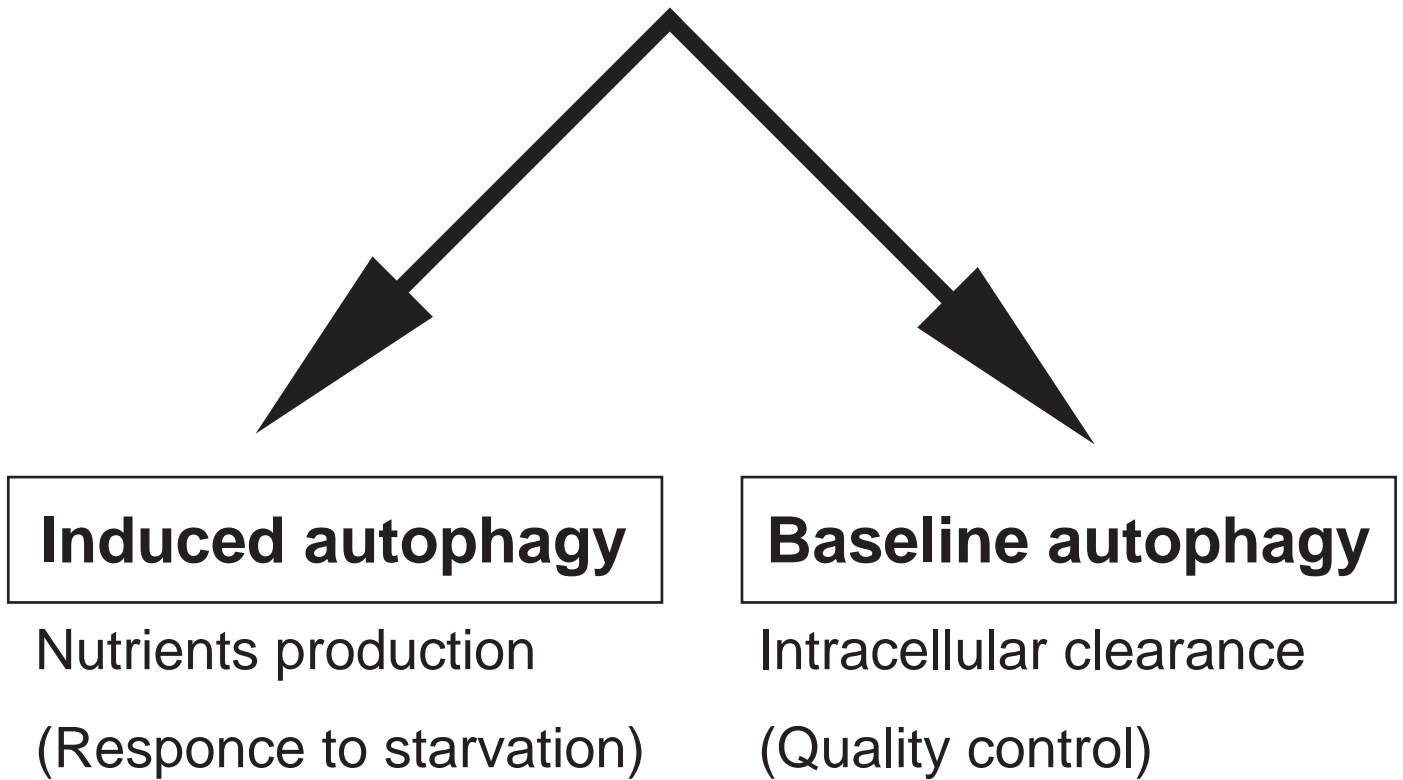


Figure 17. Roles of induced and baseline autophagy

The level of autophagy is usually low but can be upregulated by starvation such as birth and fasting. The induced autophagy is important for intracellular generation of amino acids. On the other hand, the baseline autophagy is crucial for intracellular quality control.

References

Ahlberg, J. and Glaumann, H. (1985). Uptake--microautophagy--and degradation of exogenous proteins by isolated rat liver lysosomes. Effects of pH, ATP, and inhibitors of proteolysis. *Exp Mol Pathol.* 42(1): 78-88.

Arrasate, M., Mitra, S., Schweitzer, E. S., Segal, M. R., and Finkbeiner, S. (2004). Inclusion body formation reduces levels of mutant huntingtin and the risk of neuronal death." *Nature.* 431(7010): 805-810.

Baehrecke, E. (2003). Autophagic programmed cell death in *Drosophila*. *Cell Death Differ.* 10(9): 940-945.

Bassnett, S. (2002). "Lens Organelle Degradation." *Exp Eye Res.* 74(1): 1-6.

Bjorkoy, G., Lamark, T. et al. (2005). p62/SQSTM1 forms protein aggregates degraded by autophagy and has a protective effect on huntingtin-induced cell death. *J Cell Biol.* 171(4): 603-614.

Bowen, I. D., Lewis, G. H. (1980). Acid phosphatase activity and cell death in mouse thymus. *Histochemistry* 65, 173-179.

Bursch, W., Ellinger, A., Gerner, C., and Schultze-Hermann, R. (2004). Autophagocytosis and programmed cell death. In *autophagy*, D. J. Klionsky, ed. (Georgetown, TX: Landes Bioscience)(pp. 287-303).

Clarke, P., G. (1990). Developmental cell death: morphological diversity and multiple mechanisms. *Anat Embryol (Berl).* 181(3): 195-213.

David, L. and Shearer, T. (1989). Role of proteolysis in lenses: a review. *Lens Eye*

Toxic Res. 6(4): 725-747.

De Duve, C. and Wattiaux, R. (1966). Functions of lysosomes. *Annu Rev of Physiol.* 28(1): 435-492.

Dengjel, J., Schoor, O., Fischer, R., Reich, M., Kraus, M., Muller, M., Kreymborg, K., Altenberend, F., Brandenburg, J., Kalbacher, H., et al. (2005). From the autophagy promotes MHC class II presentation of peptides from intracellular source proteins. *Proc Natl Acad Sci.* 102(22): 7922-7927.

Dice, j. F. (1990). Peptide sequences that target cytosolic proteins for lysosomal proteolysis. *Trends Biochem Sci.* 15(8): 305-309.

Doherty, F., J., Osborn, N., U., Wassell, J., A., Heggie, P., E., Laszlo, L., and Mayer, R., J. (1989). Ubiquitin-protein conjugates accumulate in the lysosomal system of fibroblasts treated with cysteine proteinase inhibitors. *Biochem J.* 263(1): 47-55.

Dunn, J. W. A. (1994). Autophagy and related mechanisms of lysosome-mediated protein degradation. *Trend Cell Biol.* 4(4): 139-143.

Fortun, J., Dunn, W. A., Jr., Joy, S., Li, J., and Notterpek, L. (2003). Emerging role for autophagy in the removal of aggresomes in schwann cells. *J Neurosci.* 23(33): 10672-10680.

Gozuacik, D., Kimchi, A. (2004). Autophagy as a cell death and tumor suppressor mechanism. *Oncogene.* 23(16): 2891-2906.

Hershko, A. and Ciechanover, A. (1998). The ubiquitin system. *Annu Rev Biochem.* 67(1): 425-479.

Heynen, M., Tricot, G., and Verwilghen, R. (1985). Autophagy of mitochondria in rat bone marrow erythroid cells. Relation to nuclear extrusion. *Cell Tissue Res.* 239(1): 235-239.

Hochstrasser, M. (1996). Ubiquitin-dependent protein degradation. *Annu Rev Genet.* 30(1): 405-439.

Ichimura, Y., Kirisako, T., Takao, T., Satomi, Y., Shimonishi, Y., Ishihara, N., Mizushima, N., Tanida, I., Kominami, E., Ohsumi, M., et al. (2000). A ubiquitin-like system mediates protein lipidation. *Nature.* 408(6811): 488-492.

Iwata, A., Riley, B. E., Johnston, J. A., and Kopito, R. R. (2005). HDAC6 and microtubules are required for autophagic degradation of aggregated huntingtin. *J Biol Chem.* 280(48): 40282-40292.

Juhasz, G., Csikos, G., Sinka, R., Erdelyi, M., and Sass, M. (2003). The *Drosophila* homolog of Aut1 is essential for autophagy and development. *FEBS Lett.* 543(1-3): 154-158.

Klionsky, D. J. (2005). The molecular machinery of autophagy: unanswered questions. *J Cell Sci.* 118, 7-18.

Kabeya, Y., Mizushima, N., Ueno, T., Yamamoto, A., Kirisako, T., Noda, T., Kominami, E., Ohsumi, Y., and Yoshimori, T. (2000). LC3, a mammalian homologue of yeast Apg8p, is localized in autophagosome membranes after processing. *EMBO J.* 19(21): 5720-5728.

Kent, G., Minick, O., Volini, F., and Orfei, E. (1966). Autophagic vacuoles in human red cells. *Am J Pathol.* 48(5): 831-857.

Kirisako, T., Ichimura, Y., Okada, H., Kabeya, Y., Mizushima, N., Yoshimori, T., Ohsumi, M., Takao, T., Noda, T., and Ohsumi, Y. (2000). The reversible modification regulates the membrane-binding state of Apg8/Aut7 essential for autophagy and the cytoplasm to vacuole targeting pathway. *J Cell Biol.* 151(2): 263-276.

Klionsky, D. J., Cregg, J. M., Dunn, J. W. A., Emr, S. D., Sakai, Y., Sandoval, I. V., Sibirny, A., Subramani, S., and Thumm, M. (2003). A unified nomenclature for yeast autophagy-related genes. *Dev Cell.* 5(4): 539-545.

Klionsky, D. J. and Ohsumi, Y. (1999). Vacuolar import of proteins and organelles from the cytoplasm. *Annu Rev Cell Dev Biol.* 15(1): 1-32.

Komatsu, M., Waguri, S., Ueno, T., Iwata, J., Murata, S., Tanida, I., Ezaki, J., Mizushima, N., Ohsumi, Y., Uchiyama, Y., et al. (2005). Impairment of starvation-induced and constitutive autophagy in Atg7-deficient mice. *J Cell Biol.* 169(3): 425-434.

Kuma, A., Hatano, M., Matsui, M., Yamamoto, A., Nakaya, H., Yoshimori, T., Ohsumi, Y., Tokuhisa, T., and Mizushima, N. (2004). The role of autophagy during the early neonatal starvation period. *Nature.* 432(7020): 1032-1036.

Laszlo, L., Doherty, F. J., Osborn, N. U., and Mayer, R. J. (1990). Ubiquitinated protein conjugates are specifically enriched in the lysosomal system of fibroblasts. *FEBS Lett.* 261(2): 365-368.

Lechler, R., Aichinger, G., and Lightstone, L. (1996). The endogenous pathway of MHC class II antigen presentation. *Immunol Rev.* 151: 51-79.

Lenk, S. E., Susan, P. P., Hickson, I., Jasionowski, T., and Dunn, W. A., Jr. (1999). Ubiquitinated aldolase B accumulates during starvation-induced lysosomal proteolysis.

J Cell Physiol. 178(1): 17-27.

McAvoy, J., Chamberlain, C., de Iongh, R., Hales, A., and Lovicu, F. (1999). Lens development. Eye. 13: 425-437.

Medina, J. M., Vicario, C., Juanes, M., and Fernandez, E. (1992). Biochemical adaptation to early extrauterine life. in Perinatal Biochemistry (eds Herrera, E & Knopp, R), 233-258.

Meijer, A. J., and Codogno, P. (2004). Regulation and role of autophagy in mammalian cells. Int J Biochem Cell Biol. 36, 2445-2462.

Melendez, A., Talloczy, Z., Seaman, M., Eskelinen, E. L., Hall, D. H., and Levine, B. (2003). Autophagy Genes Are Essential for dauer development and life-span extension in *C. elegans*. Science. 301(5638): 1387-1391.

Mizushima, N. (2004). Methods for monitoring autophagy. Int J Biochem Cell Biol. 36(12): 2491-2502.

Mizushima, N., Noda, T., Yoshimori, T., Tanaka, Y., Ishii, T., George, M. D., Klionsky, D. J., Ohsumi, M., and Ohsumi, Y. (1998). A protein conjugation system essential for autophagy. Nature. 395(6700): 395-398.

Mizushima, N., Yamamoto, A., Hatano, M., Kobayashi, Y., Kabeya, Y., Suzuki, K., Tokuhisa, T., Ohsumi, Y., and Yoshimori, T. (2001). Dissection of autophagosome formation using Apg5-deficient mouse embryonic stem cells. J Cell Biol. 152(4): 657-668.

Mizushima, N., Yamamoto, A., Matsui, M., Yoshimori, T., and Ohsumi, Y. (2004). *In vivo* analysis of autophagy in response to nutrient starvation using transgenic mice

expressing a fluorescent autophagosome marker. *Mol Biol Cell*. 15(3): 1101-1111.

Mizushima, N., Yoshimori, T., and Ohsumi, Y. (2003). Role of the Apg12 conjugation system in mammalian autophagy. *Int J Biochem Cell Biol*. 35(5): 553-561.

Mortimore, G. E., Lardeux, B. R., and Adams, C. E. (1988). Regulation of microautophagy and basal protein turnover in rat liver. Effects of short-term starvation. *J Biol Chem*. 263(5): 2506-2512.

Mortimore, G. E., Lardeux, B. R., Heydrick, S. J. (1989). Mechanism and control of protein and RNA degradation in the rat hepatocyte: two modes of autophagic sequestration. *Revis Biol Celular*. 20: 79-96.

Mortimore, G. E. and Poso, A. R. (1987). Intracellular Protein catabolism and its control during nutrient deprivation and supply. *Annual Review of Nutrition*. 7(1): 539-568.

Mortimore, G. E., Schworer, C. M. (1975). Application of liver perfusion as an in vitro model in studies of intracellular protein degradation. *Ciba Found Symp*. 75: 281-305.

Mortimore, G. E. and Poso, A. R. (1986). The lysosomal pathway of intracellular proteolysis in liver: regulation by amino acids. *Adv Enzyme Regul*. 25: 257-276.

Nakagawa, I., Amano, A., Mizushima, N., Yamamoto, A., Yamaguchi, H., Kamimoto, T., Nara, A., Funao, J., Nakata, M., Tsuda, K., et al. (2004). Autophagy defends cells against invading group A streptococcus. *Science*. 306(5698): 1037-1040.

Nimmerjahn, F., Milosevic, S., Behrends, U., Jaffee, E., M., Pardoll, D., M., Bornkamm, G., W., and Mautner, J. (2003). Major histocompatibility complex class II-restricted presentation of a cytosolic antigen by autophagy. *European Journal of Immunology*.

33(5): 1250-1259.

Nishimoto, S., Kawane, K., Watanabe-Fukunaga, R., Fukuyama, H., Ohsawa, Y., Uchiyama, Y., Hashida, N., Ohguro, N., Tano, Y., Morimoto, T., et al. (2003). Nuclear cataract caused by a lack of DNA degradation in the mouse eye lens. *Nature*. 424(6952): 1071-1074.

Ogawa, M., Yoshimori, T., Suzuki, T., Sagara, H., Mizushima, N., and Sasakawa, C. (2005). Escape of intracellular shigella from autophagy. *Science*. 307(5710): 727-731.

Ohsumi, Y. (2001). Molecular dissection of autophagy: two ubiquitin-like systems. *Nat Rev Mol Cell Biol*. 2(3): 211-216.

Onodera, J. and Ohsumi, Y. (2004). Ald6p is a preferred target for autophagy in yeast, *Saccharomyces cerevisiae*. *J Biol Chem*. 279(16): 16071-16076.

Orth, M., Cooper, J. M., Bates, G. P., Schapira, A. H. (2003). Inclusion formation in Huntington's disease R6/2 mouse muscle cultures. *J Neurochem* 87, 1-6.

Otto, G. P., Wu, M. Y., Kazgan, N., Anderson, O. R., and Kessin, R. H. (2004). Dictyostelium Macroautophagy Mutants Vary in the Severity of Their Developmental Defects. *J Biol Chem* 279, 15621-15629.

Otto, G. P., Wu, M. Y., Kazgan, N., Anderson, O. R., and Kessin, R. H. (2003). Macroautophagy Is Required for Multicellular development of the social amoeba *Dictyostelium discoideum*. *J Biol Chem*. 278(20): 17636-17645.

Paludan, C., Schmid, D., Landthaler, M., Vockerodt, M., Kube, D., Tuschl, T., and Munz, C. (2005). Endogenous MHC Class II processing of a viral nuclear antigen after autophagy. *Science*. 307(5709): 593-596.

Ravikumar, B., Duden, R., and Rubinsztein, D. C. (2002). Aggregate-prone proteins with polyglutamine and polyalanine expansions are degraded by autophagy. *Hum Mol Genet.* 11(9): 1107-1117.

Ravikumar, B., Rubinsztein, D. C. (2004). Can autophagy protect against neurodegeneration caused by aggregate-prone proteins? *Neuroreport.* 15(16): 2443-2445.

Ravikumar, B., Vacher, C., Berger, Z., Davies, J. E., Luo, S., Oroz, L. G., Scaravilli, F., Easton, D. F., Duden, R., O'Kane, C. J., and Rubinsztein, D. C. (2004). Inhibition of mTOR induces autophagy and reduces toxicity of polyglutamine expansions in fly and mouse models of Huntington disease. *Nat Genet.* 36(6): 585-595.

Sakai, Y., Koller, A., Rangell, L. K., Keller, G. A., and Subramani, S. (1998). Peroxisome degradation by microautophagy in *pichia pastoris*: identification of specific steps and morphological intermediates. *J Cell Biol.* 141(3): 625-636.

Saudou, F., Finkbeiner, S., Devys, D., and Greenberg, M. E. (1998). Huntingtin acts in the nucleus to induce apoptosis but death does not correlate with the formation of intranuclear inclusions. *Cell.* 95(1): 55-66.

Schwartz, A., L., Ciechanover, A., Brandt, R., A., and Geuze, H., J. (1988). Immunoelectron microscopic localization of ubiquitin in hepatoma cells. *EMBO J.* 7(10): 2961-2966.

Schworer, C. M., Shiffer, K. A., and Mortimore, G. E. (1981). Quantitative relationship between autophagy and proteolysis during graded amino acid deprivation in perfused rat liver. *J Biol Chem.* 256(14): 7652-7658.

Scott, R. C., Schuldiner, O., and Neufeld, T. P. (2004). Role and regulation of starvation-induced autophagy in the *Drosophila* Fat Body. *Dev Cell*. 7(2): 167-178.

Scott, S. V., Hefner-Gravink, A., Morano, K. A., Noda, T., Ohsumi, Y., and Klionsky, D. J. (1996). Cytoplasm-to-vacuole targeting and autophagy employ the same machinery to deliver proteins to the yeast vacuole. *Proc Nat Acad Sci*. 93(22): 12304-12308.

Seglen, P. O., Bohley, P (1992). Autophagy and other vacuolar protein degradation mechanisms. *Experientia*. 48(2): 158-172.

Shieh, H. L., and Chiang, H. L. (1998). *In vitro* reconstitution of glucose-induced targeting of fructose-1, 6-bisphosphatase into the vacuole in semi-intact yeast cells. *J Biol Chem*. 273(6): 3381-3387.

Takano-Ohmuro, H., Mukaida, M., Kominami, E., and Morioka, K. (2000). Autophagy in embryonic erythroid cells: its role in maturation. *Eur J Cell Biol*. 79(10): 759-764.

Takeshige, K., Baba, M., Tsuboi, S., Noda, T., and Ohsumi, Y. (1992). Autophagy in yeast demonstrated with proteinase-deficient mutants and conditions for its induction. *J Cell Biol*. 119(2): 301-311.

Taylor, J. P., Tanaka, F., Robitschek, J., Sandoval, C. M., Taye, A., Markovic-Plese, S., and Fischbeck, K. H. (2003). Aggresomes protect cells by enhancing the degradation of toxic polyglutamine-containing protein. *Hum Mol Genet*. 12(7): 749-757.

Teckman, J. H., and Perlmutter, D. H. (2000). Retention of mutant alpha 1-antitrypsin Z in endoplasmic reticulum is associated with an autophagic response. *Am J Physiol Gastrointest Liver Physiol*. 279(5): G961-974.

Tooze, J. and Davies, H. G. (1965). Cytolysome in amphibian erythrocytes. *J Cell Biol.* 24(1): 146-150.

Tsukada, M. and Ohsumi, Y. (1993). Isolation and characterization of autophagy-defective mutants of *Saccharomyces cerevisiae*. *FEBS Lett.* 333(1-2): 169-174.

Tuttle, D. L. and Dunn, W. A. (1995). Divergent modes of autophagy in the methylotrophic yeast *Pichia pastoris*. *J Cell Sci.* 108(1): 25-35.

Ueno, T. and Kominami, E. (1991). Mechanism and regulation of lysosomal sequestration and proteolysis. *Biomed Biochim Acta.* 50(4-6): 365-371.

van Leyen, K., Duvoisin, R. M., Engelhardt, H., and Wiedmann, M. (1998). A function for lipoxygenase in programmed organelle degradation. *Nature.* 395(6700): 392-395.

Walton, J. and McAvoy, J. (1984). Sequential structural response of lens epithelium to retina-conditioned medium. *Exp Eye Res.* 39(2): 217-229.

Watanabe, M., Dykes-Hoberg, M., Culotta, V. C., Price, D. L., Wong, P. C., Rothstein, J. D. (2001). Histological evidence of protein aggregation in mutant SOD1 transgenic mice and in amyotrophic lateral sclerosis neural tissues. *Neurobiol Dis* 8, 933-941.